

AD615014

RADC-TR- 64-583  
Final Report



MULTIMEGAWATT BROADBAND MICROWAVE TUBES  
AND RELATED STUDIES

TECHNICAL REPORT NO. RADC-TR- 64-583  
March 1965

COPY	2	OF	3
HARD COPY	\$ 3.00		
MICROFILM	\$ .075		

61P

DDC  
RECEIVED  
MAY 17 1965  
DDC-IRA E

Techniques Branch  
Rome Air Development Center  
Research and Technology Division  
Air Force Systems Command  
Griffiss Air Force Base, New York

ARCHIVE COPY

(X)

When US Government drawings, specifications, or other data are used for any purpose other than a definitely related government procurement operation, the government thereby incurs no responsibility nor any obligation whatsoever; and the fact that the government may have formulated, furnished, or in any way supplied the said drawings, specifications, or other data is not to be regarded by implication or otherwise, as in any manner licensing the holder or any other person or corporation, or conveying any rights or permission to manufacture, use, or sell any patented invention that may in any way be related thereto

Do not return this copy. Retain or destroy.

MULTIMEGAWATT BROADBAND MICROWAVE TUBES  
AND RELATED STUDIES

## FOREWORD

This report describes the results achieved under Contract Number AF30(602)-2575 during the third and final contract year, November 1, 1963 to October 31, 1964. Much of the work on the now expired contract will be continued under a new contract, AF30(602)-3595.

During this third contract year, the objectives of the research program were modified. Earlier, the main emphasis was on conducting theoretical and experimental investigations of generating high peak and average powers in microwave tubes over relatively broad bandwidths. While some work is continuing on this subject, the scope has been extended to include: high power broad band devices, and phase-shifter and delay-line mechanisms. The particular projects are described herein and the Table of Contents shows the project grouping under these two areas of research interest. A brief discussion of this new emphasis is presented in the Introduction.

During this contract year a total of nine reports were written and distributed, including three status reports, as follows:

- (1) F. Ivanek, "Study of Modes and Their Suppression in Broadband Periodic Structures for High-Power TWT Amplifiers," Technical Documentary Report (Microwave Laboratory Report No. 1115). Also issued as RADC-TDR-62-532.
- (2) T. Wessel-Berg, "An Analysis of Orbit Pumping Phenomena in Quadrupoles," Technical Documentary Report (Microwave Laboratory Report No. 1130). This report was also issued by RADC as RADC-TDR-64-82.
- (3) H. L. Stover, "Microwave and Electron Beam Interactions with a Finite Plasma," Technical Documentary Report (Microwave Laboratory Report No. 1140). This report was also issued by RADC as Technical Documentary Report No. RADC-TDR-64-117.
- (4) Quarterly Status Report No. 9, for 1 November 1963 to 31 January 1964 (Microwave Laboratory No. 1143). This report was not printed as an RADC TDR.
- (5) A. J. Bahr, "On the Analysis and Suppression of Oscillations in High-power Traveling-wave Tubes," Technical Documentary Report (Microwave Laboratory Report No. 1147). This report was also issued by RADC as Report No. RADC-TDR-64-172.
- (6) C.C. Lo, "Studies of the Effect of Circuit Tapering on TWT Performance," Technical Documentary Report (Microwave Laboratory Report No. 1155). This report was also issued by RADC as RADC-TDR-64-322.

- (7) Quarterly Status Report No. 10, for 1 February to 30 April 1964 (Microwave Laboratory Report No. 1178). Also issued as RADC-TDR-64-357.
- (8) Bas Hoeks, "Space-charge Waves in an Accelerated Parallel-flow Electron Beam in a Constant Magnetic Field," Technical Documentary Report (Microwave Laboratory Report No. 1205). Also issued as RADC-TDR-64-404.
- (9) Quarterly Status Report No. 11, for 1 May to 31 July 1964 (Microwave Laboratory Report No. 1224). Also issued as RADC-TDR-64-465.

This Annual Report summarizes the information presented in all of the above nine reports and describes the work done in the last quarterly period as well.

During the course of this contract year, some projects were terminated and some new projects were begun. Such changes were described in the appropriate status reports. At the time of this present report, six projects were active:

- I. Extended-interaction klystrons
- II. Centipede TWT
- III. Transverse-wave studies
- IV. Whistler mode propagation in solids
- V. Carrier wave propagation in semiconductors (Gunn oscillations)
- VI. Acoustic wave devices.

The Responsible Investigator for this contract is Professor Marvin Chodorow.

The RADC Project Engineer was Lt. William Wilson (EMATE). The Project Number was 5573 and the task Number 557303.

This technical report has been reviewed and is approved.

Approved: *Arthur J. Frohlich*  
ARTHUR J. FROHLICH  
Chief, Techniques Branch  
Surveillance & Control Division

Approved: *Thomas S. Bond, Jr*  
THOMAS S. BOND, Jr  
Colonel, USAF  
Surveillance & Control Division

FOR THE COMMANDER: *Irving J. Gabelman*  
IRVING J. GABELMAN  
Chief, Advanced Studies Group

## ABSTRACTS

### I. EXTENDED-INTERACTION KLYSTRONS

The small-signal performance of a three-cavity extended-interaction klystron, operating in conjunction with the electron stick, at 1100 Mc, and with beam voltages near 25 kV, is in good agreement with the theory. Saturation measurements are in progress, with the object of finding the best interaction length and loading of the output region for greatest power-bandwidth.

### II. CENTIPEDE TWT

A centipede propagating structure has been operated as a high power traveling wave tube, using the electron stick to provide the electron beam, at beam voltages of 100 kV. Use of the stick allows direct measurements to be made of amplitude and phase of the fields within the coupled cavities by means of direct field probing. A space-charge wave theory, and an improved equivalent circuit for this system, have been derived, and the experimental results are in good agreement with this theory. The experimental work is nearly completed, and a technical report is in preparation.

### III. TRANSVERSE-WAVE STUDIES

The study of transverse wave propagation on accelerated streams has established some useful information on the transformation properties of accelerated regions. The analytical treatment involves a number of approximate methods for obtaining asymptotic solutions. In particular, the quasi-static, thin-beam approximation has been used. The results are summarized in the present report.

#### IV. WHISTLER MODE PROPAGATION IN SOLIDS

The purpose of this study is to investigate wave propagation through solid state material which depends on plasma effects resulting from the collective motion of the conduction electrons. This project has been active for one quarter, during which time preliminary calculations have been made on the propagation of Whistler modes in indium antimonide. Samples have been obtained, and an initial experiment is being set up for operation in the high microwave frequency range.

#### V. CARRIER WAVE PROPAGATION IN SOLIDS

A study of the Gunn effect and related waves which can propagate through a semiconductor has been started. Gallium arsenide, indium phosphide, and other semiconductor materials have been obtained for this purpose. Oscillations have already been observed with our first Gunn diodes made in this laboratory. A theory for this effect which depends on saturation of the current-voltage characteristic due to optical phonon interactions has been formulated, which indicates that waves can propagate through a saturated semiconductor without loss. However, only a small negative resistance effect, insufficient to explain Gunn oscillations, is predicted. Other theoretical causes for the negative resistance are presently being examined.

#### VI. ACOUSTIC WAVE DEVICES

Facilities are being established for the fabrication of new types of transducers, particularly thin-film types, for the coupling of electromagnetic energy into microwave acoustic waves. The objective is to experimentally test new approaches for the reduction of coupling loss, which is of utmost importance at this time to the development of practical microwave time and phase delay systems and other devices employing acoustic waves. Several transducers employing magnetostrictive nickel films have been fabricated and tested, and initial results on the dependence of coupling loss on fabrication parameters are presented.

TABLE OF CONTENTS

	Page
Preface . . . . .	iii
Abstracts . . . . .	vi
Introduction . . . . .	1
Part I: High power broad band devices	
I. Extended-interaction klystrons . . . . .	5
II. Centipede TWT . . . . .	15
Part II: Phase-shifter and delay-line mechanisms	
III. Transverse-wave studies . . . . .	22
IV. Whistler mode propagation in solids . . . . .	37
V. Carrier wave propagation in semiconductors (Gunn oscillations) . . . . .	39
VI. Acoustic wave devices . . . . .	43

## INTRODUCTION

The primary objective of this program originally was to investigate methods of generating high peak and average powers in the microwave regions over relatively broad bandwidths. By this has been implied typical values which we might quote as 10 mW of peak power, 30 kW of average power, and 10 to 20% bandwidth in the S-band region. Most of our individual projects in the past have been aimed at these kinds of objectives, and, in particular, have been concerned with understanding the properties of either traveling wave tubes or klystrons which could reach these objectives, while also attempting to resolve some of the difficulties which existed in such devices. Over the years, considerable progress has been made in achieving the aims of the program, and in the last year or so a considerable part of our effort has been aimed at looking at instabilities in traveling wave tubes, methods of avoiding them, and to some extent, at methods of extending the bandwidth of both traveling wave tubes and some special forms of klystrons. This has still represented a considerable portion of the program over the past year. However, as radar system objectives and approaches have changed, the objectives of our own program have also changed. In particular, radar systems have been trending largely into phased arrays, and these in turn depend heavily on the use of phase shifters and delay lines with electronically controllable characteristics, good power handling capabilities, and large variation in the phase shift possibilities. The program has followed these changes in radar design, and a good portion of it has been shifted over into investigating various novel mechanisms and devices which might be particularly of value in phase shifting. Hence the individual projects represent the closing stages of investigations aimed at our earlier objectives, plus the beginning stages of investigations which are aimed at these new objectives directed towards phased arrays.

In the first category, that is, projects concerned with relatively high power broadband devices, we can list two, both of which are concerned with investigating some aspect of broadband high power devices. Both utilize an experimental apparatus which has been developed in our laboratory, called the electron stick. This is a long, hollow glass cylinder with a cathode and collector, and which is lined with a very fine, closely spaced helix. This permits us to transmit a high-voltage, high-current beam along the axis of the glass cylinder without charging the walls, and permits the placing of interaction structures of various kinds on the outside of the glass cylinder. Thus the electron beam is in the vacuum, the rf structures are outside the vacuum and can be modified at will, and measurements can be made of rf field distributions under operating conditions which would not be possible if the rf structure were also part of the vacuum. The presence of the glass cylinder, and of the closely spaced tungsten helix in the interior which prevents the charging of the glass, cause a perturbation in the interaction between the beam and the exterior circuits which is quite small and calculable. The electron stick has been used, first, in a program investigating extended-interaction klystrons which is described in the body of the report. The extended-interaction klystron, which was first invented and developed in our laboratory, uses resonant lengths of a propagating circuit as klystron cavities; it can be shown that such cavities can exceed the gain bandwidth characteristics of conventional klystron cavities by a large factor. This was originally demonstrated in this laboratory and has been used extensively in various industrial laboratories. Most recently, the most unusual results have occurred in a pulsed X-band program also sponsored by RADC. In spite of the excellent achievements obtained with this circuit, there is still a great deal about the performance characteristics which is not known. In particular, it is not known how the efficiency and the bandwidth of the distributed interaction circuit vary with electrical length under large signal conditions, although remarkable efficiencies and bandwidth have been achieved. It is of importance to make a systematic investigation of the behavior, and of the effect of length on the efficiency and bandwidth. There is

a theory covering the bandwidth properties which is probably reliable, but there is not very much in the way of theory concerning the large signal efficiency. The variation of efficiency with length for an extended-interaction cavity used as an output circuit will be determined here by the electron stick investigations of distributed interaction klystrons which are described in Part I. Part II describes the use of the stick in conjunction with a propagating circuit, namely the centipede, which has already been shown to give the greatest bandwidth of any high powered circuit devised up to now. In this experiment an attempt has been made to determine the variation of the field configuration along the circuit by actually probing the cavities. In particular, it was hoped to find out how these vary under large signal conditions and also at frequencies near the band edge, where instabilities occur. For technical reasons having to do with the nature of the stick, some of these objectives, particularly large signal objectives, have not been achieved. However, we have been able to get considerable information about the behavior of the signal in a high power traveling wave tube of this kind, and to develop a theory using equivalent circuit concepts which is capable of giving better theoretical results than the previous circuit models.

These are the only two programs which are relevant to high power wide band devices. The remainder of our activities are concerned with looking at mechanisms and possible devices which might be suitable for phase shifters and delay lines. The first of these is aimed at using electrons in magnetic fields as a delay mechanism. As a preliminary to this, we have been looking at some problems of space charge waves in accelerated electron beams in a constant magnetic field. This is largely theoretical and, as has been stated already, is really a preliminary to some more directly applicable work on delay line mechanisms. Another project which is aimed at possible delay line devices uses semiconductor plasmas. It is known that certain kinds of waves will propagate in the plasma of a semiconductor. In particular, under certain conditions involving a suitable magnetic field and choice of material, one can get the analog of the Whistler mode of propagation such as occurs

in the ionosphere, with, of course, very different numerical constants specifying the medium. In a solid this is known as a helicon wave. Its interest for delay lines is that it is an extremely slow wave and can also be quite lossless. The magnetic field in this case is applied externally; it is conceivable that one can use the field to either vary the delay or the direction of propagation of the wave, with an obvious application to either microwave switching or delay lines. It is also possible that one might be able to achieve electronic control by applying dc electric fields which cause motion of the carriers, and interaction between moving carriers and helicon waves may provide amplification or control of phase characteristics. Another related investigation is aimed at identifying the mechanisms involved in oscillations in semiconductors known as Gunn oscillations. Since these are known empirically to depend on the transit time of the carriers, it is possible that a complete understanding of the oscillation mechanism may also lead to an amplification mechanism and possibly to a controllable delay mechanism. At the moment, we are investigating Gunn oscillations experimentally in some semiconductors, and also some theoretical work is underway to attempt to explain them, which would of course be necessary for utilization in the ways we have mentioned.

Finally, the last major approach to the delay line problem is through the use of high frequency acoustic waves in various solids. Propagation of such waves has been measured in this laboratory. For some materials the attenuation is found to be quite low. It is also possible, by use of acoustic amplifiers using the piezoelectric effect in semiconductors, to produce amplification of such acoustic waves. The same mechanism as used to produce amplification, namely interaction with charge carriers, can under other circumstances control the phase velocity, and this would also be a possible avenue to devices with electronically controllable phase and amplitude characteristics, and with delay times determined by acoustic velocities which are quite low. The principle effort now is concerned with the transducer problem of launching such acoustic waves; there are various approaches involving principally thin films which are under way in our laboratory. Some details of all of these topics are given in the body of this report.

## PART I: HIGH POWER BROADBAND DEVICES

### I. EXTENDED-INTERACTION KLYSTRONS

(M. Chodorow,\* B. Kulke)

#### A. INTRODUCTION

The primary purpose of this project has been the investigation of the maximum gain bandwidth product and conversion efficiency which can be achieved in an extended-interaction klystron, with cavities consisting of resonated sections of slow-wave structure. In particular, the dependence of gain-bandwidth and efficiency on resonator length, on  $M^2 R_{sh}/Q$ , and on loading conditions was to be determined. This problem has been approached in several steps, the last of which is currently awaiting completion.

The first of these steps was the detailed investigation of a high-power plane slow-wave structure, i.e., the stub-supported meander line, which held some promise of yielding a relatively high value of  $R_{sh}/Q$  when used as a cavity resonator. The results of this work have been summarized earlier.<sup>1</sup> It was found that in order to gain any advantage from the use of this structure, a planar beam would be required. However, since only a cylindrical beam was readily available (see below), the stub-supported meander line was dropped from consideration as a possible interaction structure.

The second step involved the design, construction, and evaluation of a three-cavity extended-interaction klystron operating near 100 kV at a frequency of 2800 Mc. This design was largely governed by the available experimental vehicle, i.e., the electron stick, which is a vertical, three-quarter-inch diameter, thin-walled, evacuated glass tube containing a half-inch diameter electron beam. The beam is confined by a longitudinal

---

\* Project Supervisor

magnetic field generated by a stack of coils with a five-inch inner diameter. The structure to be tested is lowered concentrically into the annular space between the glass tube and the coils, without any need for further evacuation. Pertinent design and performance data for this tube have been given earlier.<sup>2,3</sup>

Since, in view of the objectives as stated, the performance parameters of the output cavity were of greatest interest, the S-band tube was designed as a hybrid device with only the output cavity operating as a distributed interaction system, but with the input and idler cavities designed as conventional "narrow-gap" reentrant cavities. The output cavity utilized a resonated section of stub-supported ring-bar structure with its length variable from  $\pi$  to  $5\pi$  radians; this section was closely coupled at one end to a reduced-height waveguide. The input and idler cavities were plunger-tuned over a ten percent bandwidth so that they could effectively simulate a wide-band, stagger-tuned bunching section, with overall bandwidth then determined only by the output cavity. Test results obtained with this tube proved to be inconclusive because the performance was severely limited, especially for the longer (and more interesting) output interaction lengths, by regenerative oscillation in adjacent axial modes, parasitic oscillations peculiar to the electron stick, and the large values of  $\gamma a$  imposed at S-band frequencies by the inherent physical separation of the glass-enclosed beam from the slow-wave circuit.

The third step, intended as a refinement on the second step, consisted in the design, construction, and evaluation of a three-cavity extended interaction klystron operating near 25 kV at a frequency of 1100 Mc.<sup>4,5,6</sup> The lower operating voltage of this tube is designed to simplify the suppression of parasitic beam oscillations and of rf breakdown under saturated-beam conditions; the lower operating frequency implies a smaller  $\gamma a$  and, hence, greater field uniformity and interaction impedance. All three cavities utilize simple resonated ring-bar structures which at one end make ohmic contact to modified BNC connectors serving as couplers. The input and idler cavities are again made tunable over a ten-percent range; this is achieved by a novel means of variable capacitive loading of the circuit. The length of output cavity can be varied from one to

to five resonant half-wavelengths, with provision for attaching a coupler at either end of the cavity, for all lengths. The value of  $M^2 R_{sh}/Q$ , which is the relevant figure-of-merit for the performance of a klystron cavity, is about 110 ohms for the input and idler cavities (length  $2\pi$  radians) and about 240 ohms for the maximum-length output cavity (length  $5\pi$  radians); clearly, these values improve on those typical of narrow-gap cavities by a factor of two or three.

The problem of suppressing the parasitic oscillations peculiar to the electron stick has been solved in a manner consistent with the use of the close-spaced ring-bar circuit as a slow-wave structure, by wrapping the entire electron stick with a directionally resistive mylar material. This material presents only moderate and purely ohmic loading to the circuit, but completely suppresses the parasitic beam oscillation at least up to a beam voltage of 50 kV.

Regenerative oscillation of the individual cavities in axial modes adjacent to the design mode is prevented by selective internal ohmic loading of the radial electric fields near the slow-wave structure. The rf breakdown within the output cavity has been remedied successfully by immersion in a sulfur-hexafluoride atmosphere, and during trial runs saturation power levels of near 40 kW output have been achieved. Calibrated variation of the external load on the output cavity is achieved by adding a susceptance, i.e., a stub tuner, at a distance near  $\lambda g/8$  from the detuned-short position; by this method,  $Q_{ext}$  can typically be varied over a ten-to-one range.

## B. CURRENT STATUS

After ascertaining the stable operation of the L-band klystron, we have carried on beam-testing of the tube over the past few weeks. An observed frequency-dependent instability of the output signal, which last quarter had been tentatively (and erroneously) identified as being due to feedback between cavities, was shown to be caused actually by rf breakdown in the idler cavity which occurs when the tuning motion in effect narrows the gaps in that cavity. This difficulty occurs only at

power levels well into the saturation region, and can also be remedied by  $SF_6$  quenching, if necessary.

Although the primary objectives of this experiment deal with tube performance at saturation power levels, investigation of small-signal operation was felt to be essential as well, both to verify the validity of the theory in the electron-stick environment, especially for cavity lengths longer than  $2\pi$ , and as a calibration of our measurement techniques. The simplest application of the theory is in the prediction of beam-loading conductance; also, an accurate knowledge of this quantity is essential for the prediction of small-signal gain. Consequently, beam-loading conductance was measured. This was done by comparing the power reflected from the cavity with the beam off to that with the beam on. The measured results were compared to the values calculated on the basis of the axial field distributions measured earlier, and reasonable agreement was found (see Figs. 1 and 2). The fact that agreement is better for the two-cavity averages of Fig. 1 than for the single-cavity data of Fig. 2 indicates some scalloping of the dc beam, the effect of which is cancelled out by averaging over the axially separated buncher cavities.

The small-signal gain was also measured for a representative case (output cavity adjusted to length  $3\pi$ , with coupler simply terminated), and is compared with the theoretical prediction in Fig. 3; the 3 dB discrepancy is probably due primarily to the error in the prediction of beam-loading conductance which is evident from Fig. 2. The steep rise in gain vs voltage is due to the rapid increase of negative beam loading in the input cavity and the consequent decrease in total shunt conductance in that cavity, which is always stub-tuner-matched to the driving-signal generator. A more detailed discussion of these results, and of the measuring technique used to obtain them, will be presented in the final report on this project, which is in preparation. The essential point here is that an important part of the small-signal theory has been verified for this tube, thus establishing this theory both as a guideline and as a calibration standard for the purely experimental analysis which is to follow.

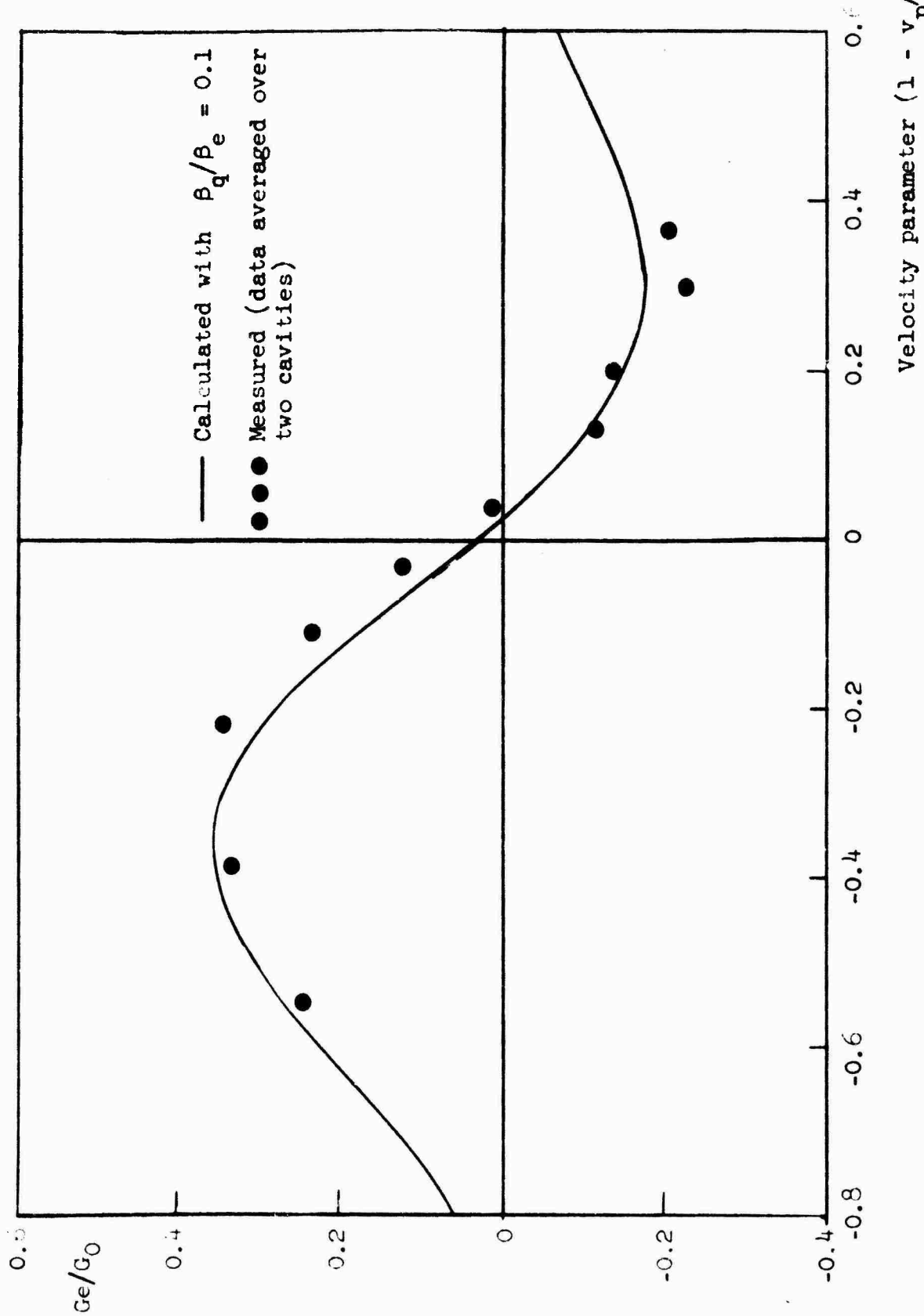


FIG. 1--Normalized beam-loading conductance,  $G_e/G_0$  for the buncher cavities (length  $2\pi$ ).

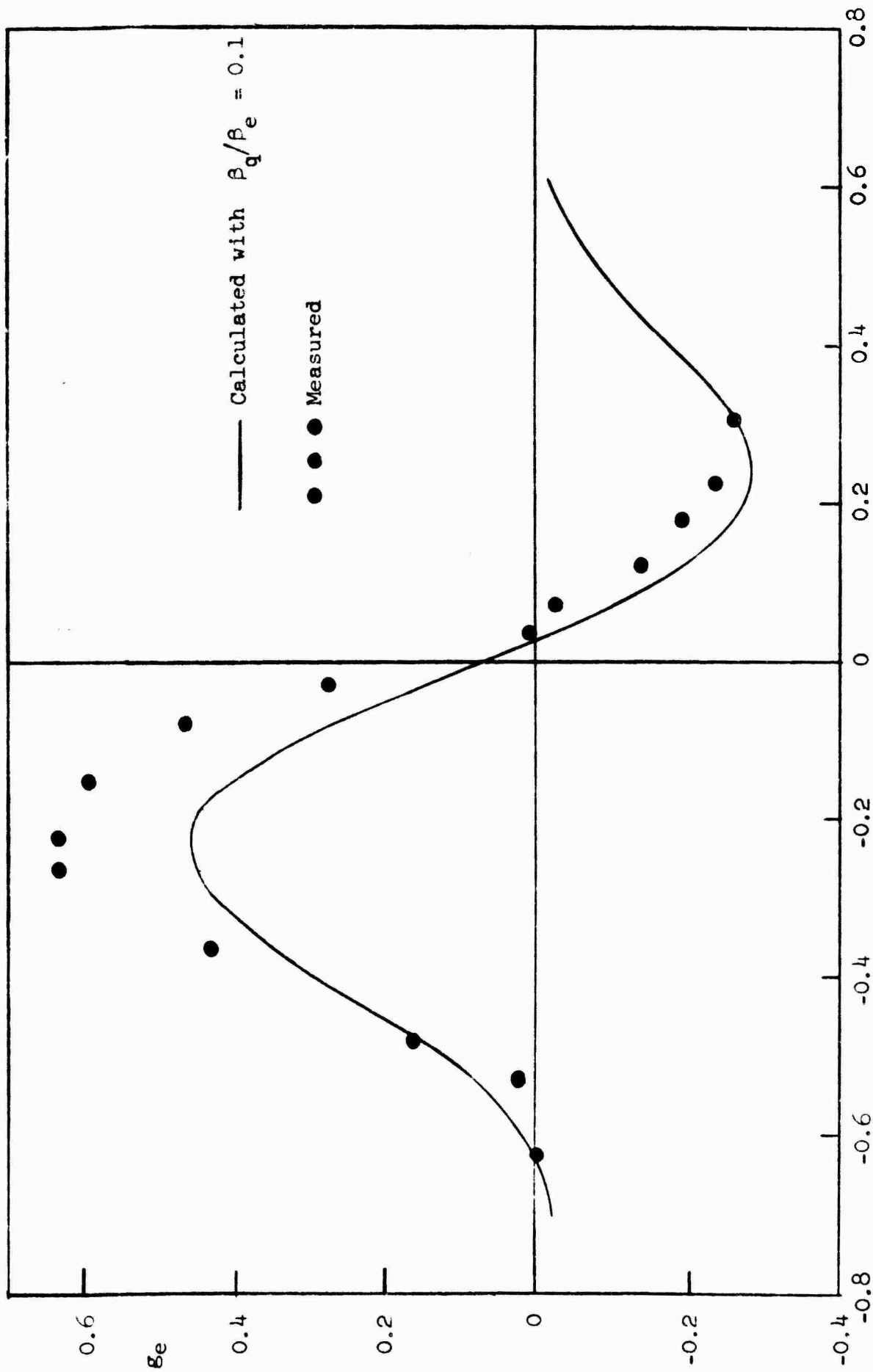


FIG. 2--Normalized beam-loading conductance,  $G_e/G_0$  for the output cavity (length  $3\pi$ ). Velocity parameter ( $1 - v_p/u_0$ )

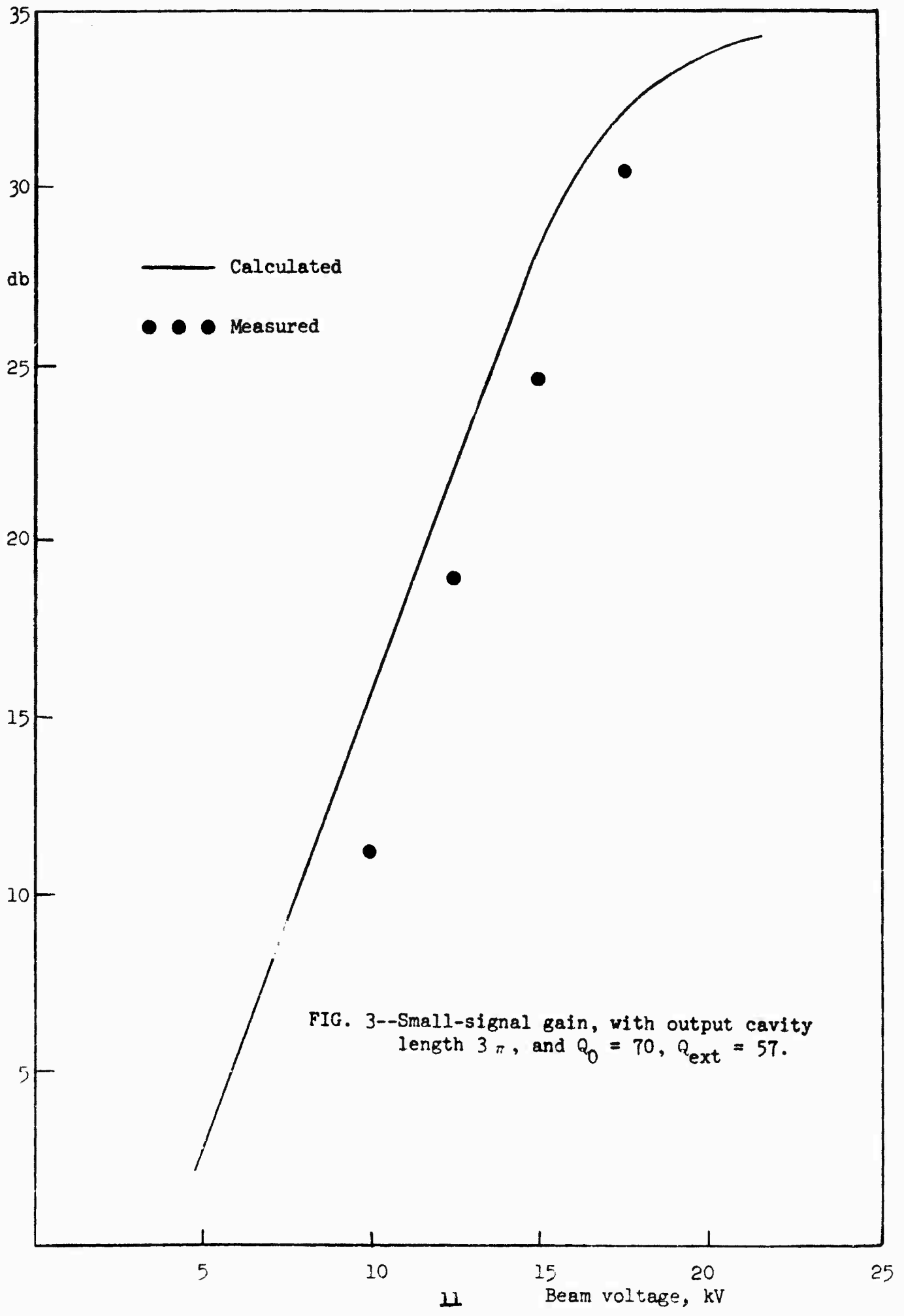


FIG. 3--Small-signal gain, with output cavity length  $3\pi$ , and  $Q_0 = 70$ ,  $Q_{ext} = 57$ .

### C. FUTURE WORK

With the small-signal performance reliably predicted, we are now proceeding to the main, and final, objective of the experimental program, i.e., an empirical evaluation of power-bandwidth and efficiency under saturated conditions as a function of output cavity length, loading, and synchronism conditions.

A typical set of results is presented in Fig. 4: for a given length of the output cavity, with a given  $Q_{\text{ext}}$ , the power output or efficiency and the 3 dB bandwidth are measured under saturated conditions, with the input cavity matched to the generator and the idler cavity tuned for maximum power output at each frequency of measurement. The nominal efficiency observed is relatively low because here the rf power absorbed by the internal losses of the output cavity nearly equals the power coupled out. However, the heavy internal loading represents a situation dictated by the experimental environment rather than a basic limitation of this type of tube, so that the actual efficiency should be assessed at nearly double the value measured.

Measurements of this type are now being made and are expected to yield, as a final result of this project, information on the optimum interaction length and the best loading conditions for greatest efficiency and power-bandwidth.

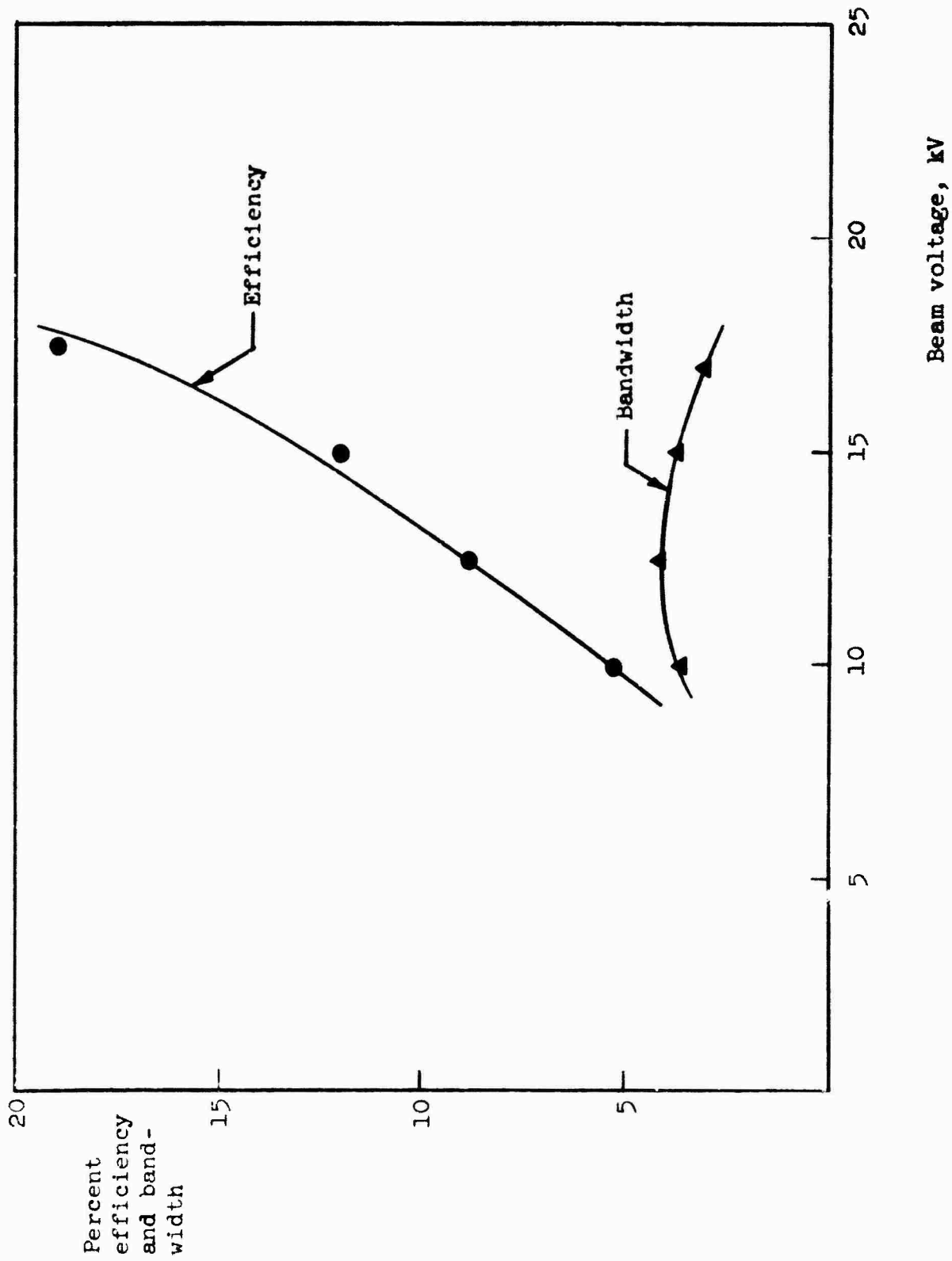


FIG. 4--Saturation efficiency and bandwidth (Output cavity length  $3\pi$ , with  $Q_0 = 70$ ,  $Q_{ext} = 57$ ).

#### REFERENCES FOR PART I

1. First Annual Report for Contract AF 30(602)-2575, Microwave Laboratory Report No. 937, Stanford University (December 1962) pp. 60-75.
2. Quarterly Status Report No. 7 for Contract AF 30(602)-2575 Microwave Laboratory Report No. 1080, Stanford University (September 1963).
3. Second Annual Report for Contract AF 30(602)-2575, Microwave Laboratory Report No. 1116, Stanford University (October 1963).
4. Quarterly Status Report No. 9 for Contract AF 30(602)-2575, Microwave Laboratory Report No. 1143, Stanford University (March 1964) pp 21-24.
5. Quarterly Status Report No. 10 for Contract AF 30(602)-2575, Microwave Laboratory Report No. 1178, Stanford University (June 1964) p. 31.
6. Quarterly Status Report No. 11 for Contract AF 30(602)-2575 Microwave Laboratory Report No. 1224, Stanford University (September 1964), pp. 15 - 18.

## II. CENTIPEDE TWT

(D. K. Winslow,\* T. Reeder)

### A. INTRODUCTION

The objective of this project is to study the interaction between the electron beam and slow-wave circuit in a high power traveling-wave tube. The centipede slow-wave circuit, a coupled cavity structure, is used in this study. In particular, the centipede has been chosen because it has proven to be one of the most satisfactory slow-wave structures for a high power TWT. The method of investigation is to measure the amplitude and phase of the fields in each centipede cavity while the centipede is mounted on the electron stick and is being operated as a TWT. Measurements over a particular region are possible, such as at a sever and in the output section of the tube. The results of this study are of the utmost value in optimizing the many parameters affecting the beam-circuit interaction.

### B. DISCUSSION

The bulk of the experimental and theoretical work on this project has been completed, and a comprehensive report is being written which describes the important results obtained by this study. Since this report should be available for distribution in the near future, only a summary of the project work will be given here.

#### 1. Experimental Work

The experimental measurement of field amplitude and phase in each coupled-cavity of the centipede tube was described in previous reports.<sup>1,2</sup>

---

\* Project Supervisor.

A small loop probe was constructed which could be coupled to be rf magnetic field inside each cavity by small slots, as shown in Fig. 1. The amplitude and phase of the fields sampled by this probe were measured by standard microwave techniques at a location remote from the tube. The mechanical construction and operation of the probe were greatly simplified due to the fact that the measurements were made with the centipede waveguide mounted on the electron stick. With this setup the centipede circuit and field probe were outside the electron beam vacuum envelope, making adjustment and operation of the probe relatively easy.

Measurements of field amplitude and phase were first made with the electron beam turned off so that the cold attenuation and  $\omega$ - $\beta$  characteristics of the centipede circuit could be obtained. These cold measurements were the first to be reported in which a movable field probe was used to sense the amplitude and phase changes over the length of a coupled cavity waveguide. As described in Report No. 10,<sup>2</sup> the  $\omega$ - $\beta$  data were quite accurately obtained, even in the presence of the loss added to the centipede circuit and electron stick for oscillation suppression. The well-known perturbation method<sup>3</sup> of obtaining  $\omega$ - $\beta$  data was useless for measuring such a high loss circuit.

Hot test measurements with an accelerating voltage of 100 kV and pulsed beam current of 61 amps showed that the rate of growth and phase shift per cavity of the growing wave could be accurately measured with the experimental setup. A discussion of the hot test data was given in Report No. 10.<sup>2</sup>

## 2. Theoretical Work

A small signal wave theory description of the interaction of an electron beam with a chain of coupled-cavity resonators has been derived. The theory includes the effect of the two fundamental space charge waves of the beam interacting with the forward and backward traveling waves of the circuit. An equivalent circuit which is an accurate representation of the  $\omega$ - $\beta$ ,  $E^2/W$ , and loss characteristics of the centipede is used to represent the coupled cavity circuit. The development of this equivalent circuit has been given in previous reports.<sup>4,5,6</sup> As far as the

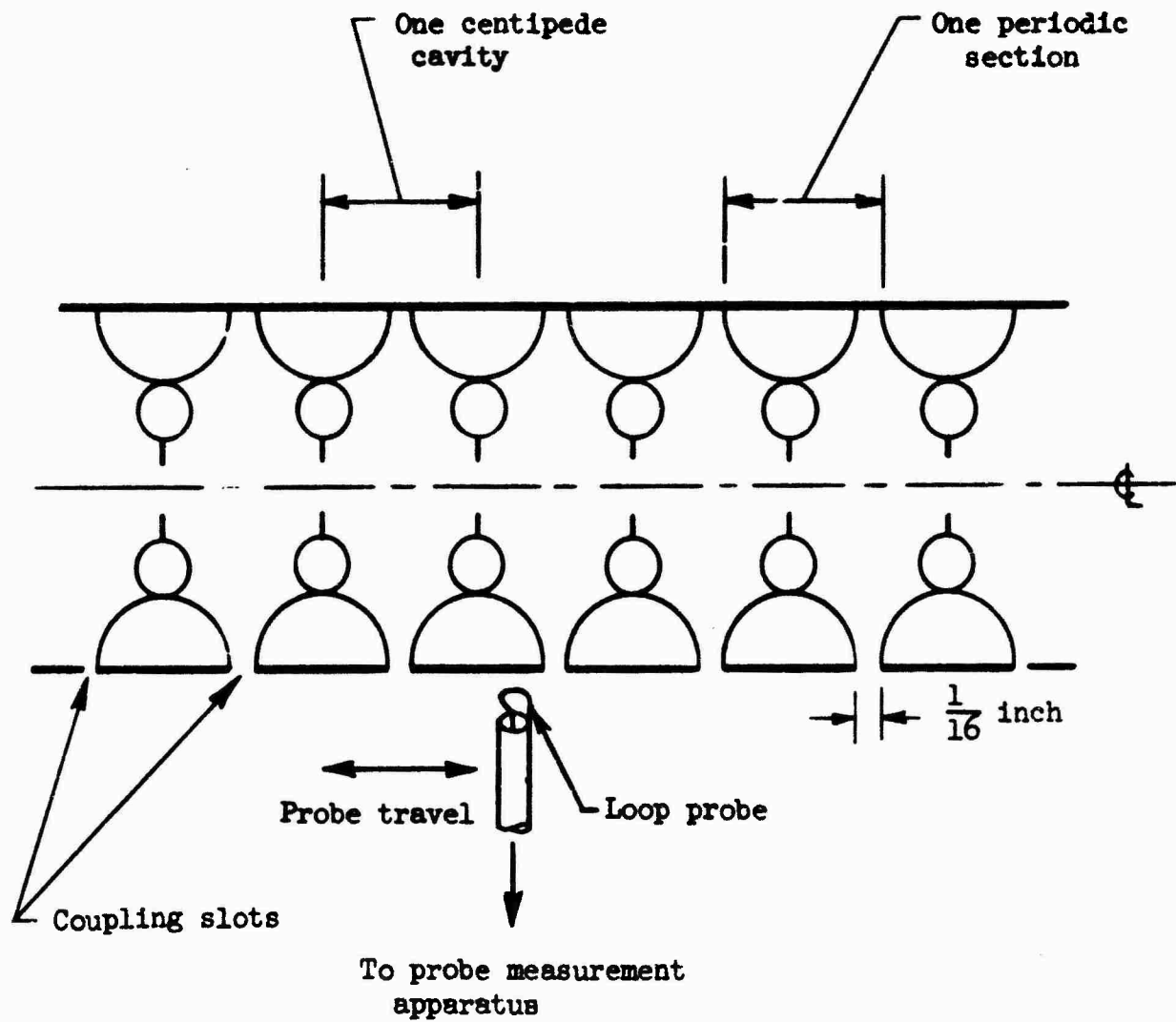


FIG. 1--Cross-sectional view of the centipede structure showing field probe and coupling slot location.

electron dynamics are concerned, the theory assumes that each centipede cavity is a long transit angle planar gap and that there is no drift space between cavities. Under small signal conditions a dispersion equation can be derived for the system consisting of the electron beam and the coupled-cavity equivalent circuit which shows that four allowed waves may propagate on the system. The relative excitation of these four waves is determined by an analysis of the boundary conditions for the beam and equivalent circuit. The loop current flowing in each coupled cavity of the equivalent circuit is defined as a quantity proportional in amplitude and phase to the magnetic field at the wall of the corresponding cavity of the actual centipede circuit. Thus, when the theory is used to calculate the relative amplitude and phase of the loop currents for the equivalent circuit-electron beam system, these amplitudes and phases should be the same as the experimentally measured field amplitude and phase at each cavity. As an example of how well the calculated and measured amplitudes and phases agree, consider Figs. 2 and 3. The experimentally measured amplitudes and phases are the same hot test data described in Report No. 10.<sup>2</sup> Note that the calculated amplitudes and phase are in good agreement with the experimental data. The parameters of the equivalent circuit were adjusted so that the cold test data of the centipede were most accurately represented at the frequency shown, 2800 Mc. Since the equivalent circuit is less accurate at other frequencies, the agreement between calculated and measured data is not as good at frequencies away from 2800Mc. However, the qualitative behavior of the electron beam-equivalent circuit system was seen to be the same as the measured behavior of the centipede TWT for frequencies covering the entire fundamental passband, even at frequencies near the band edge.

The accuracy of the theory just outlined, as well as additional discussion of the wave description of the centipede TWT, is given in the comprehensive technical report now in preparation.

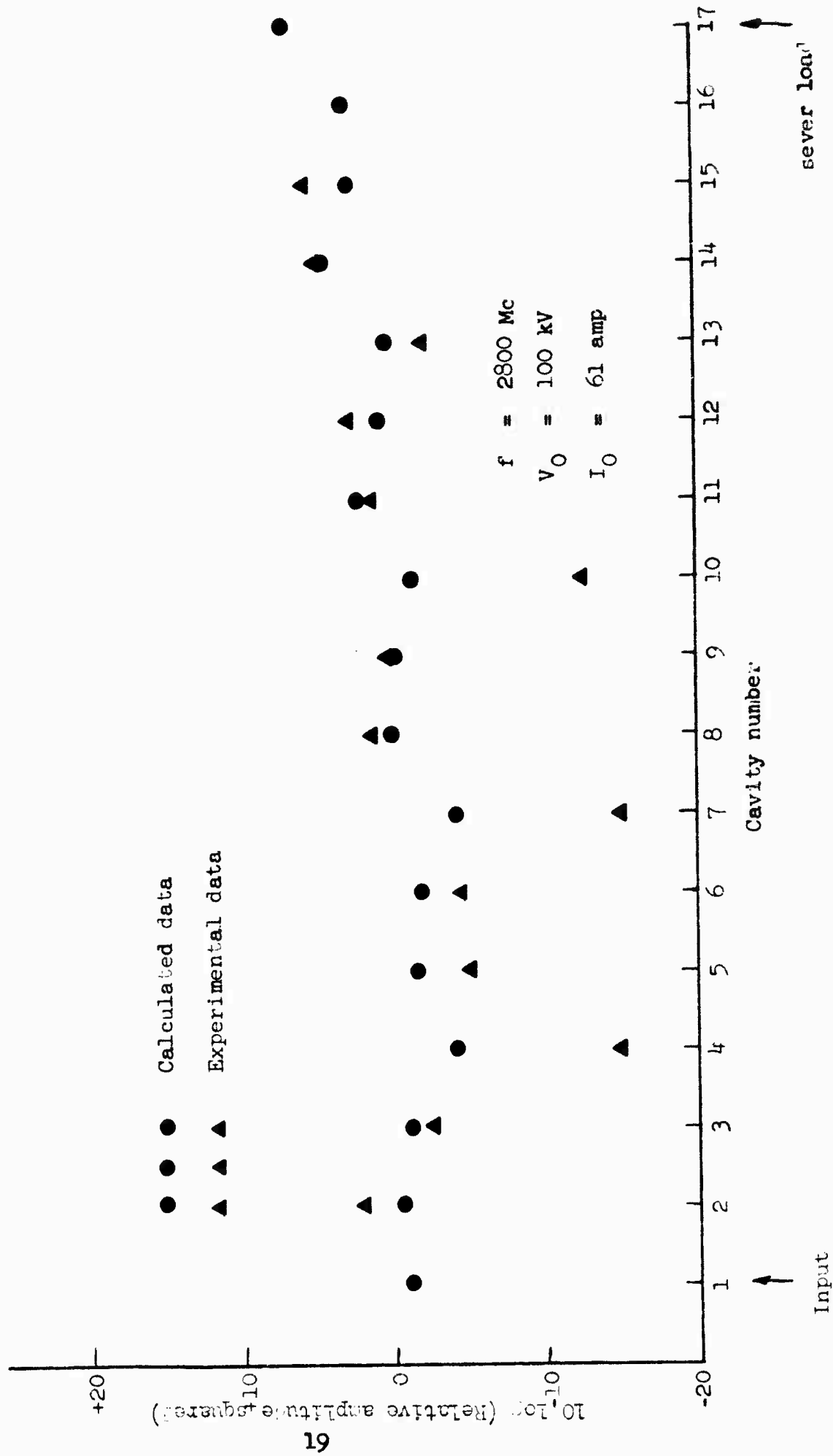


FIG. 2--Cavity field amplitude plot for the centipede TWT.

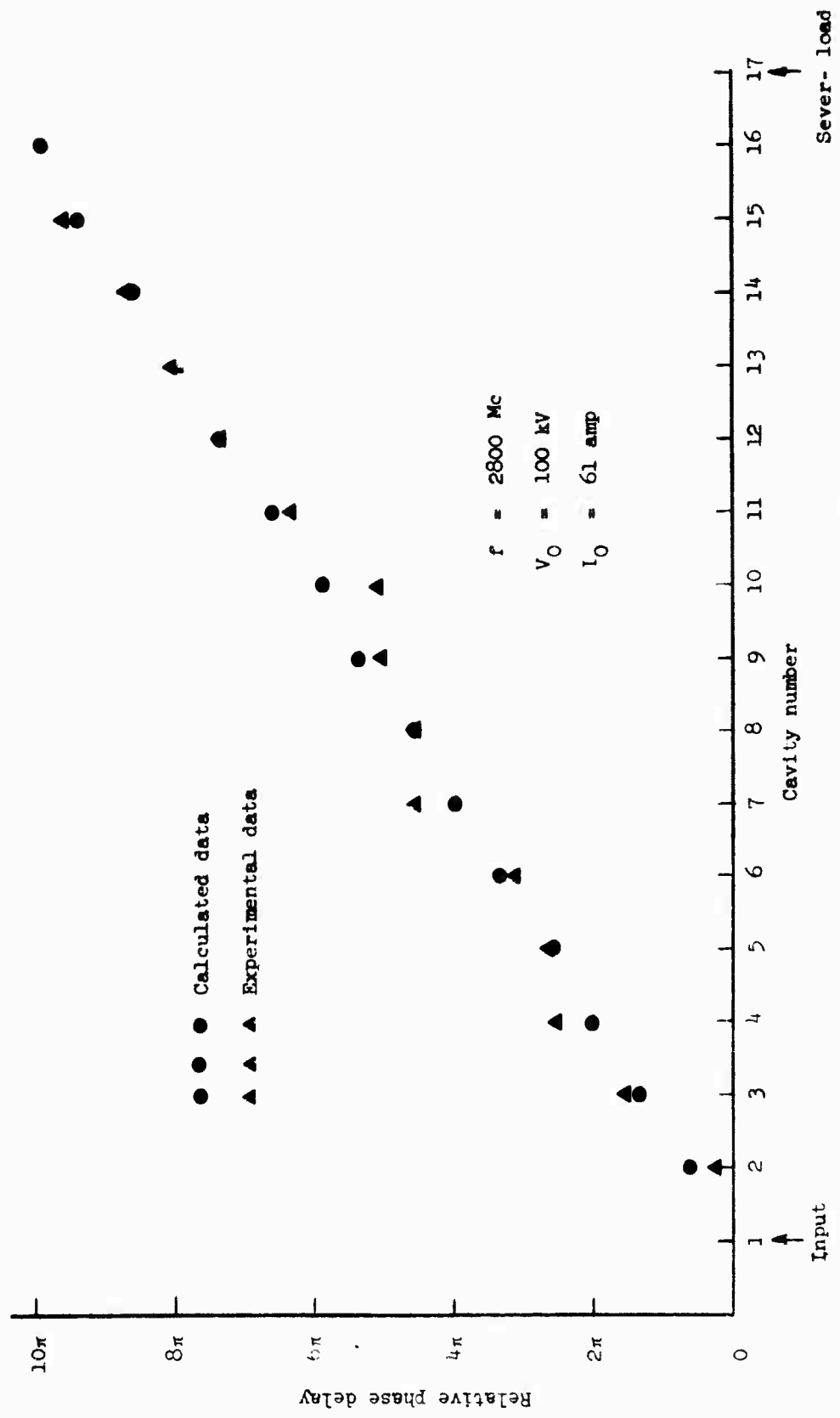


FIG. 3--Cavity field phase plot for the centipede TWT.

## REFERENCES FOR PART II

1. Quarterly Status Report No. 7 for Contract AF 30(602)-2575, Microwave Laboratory Report No. 1080, Stanford University (September 1963).
2. Quarterly Status Report No. 10 for Contract AF 30(602)-2575, Microwave Laboratory Report No. 1178, Stanford University (June 1964).
3. Nalos, E. J., "Measurement of Circuit Impedance of Periodically Loaded Structures by Frequency Perturbations," Proc. IRE 42, 1508-1511 (October 1954).
4. Quarterly Status Report No. 6 for Contract AF 30(602)-2575, Microwave Laboratory Report No. 1037, Stanford University (April 1963).
5. Second Annual Report for Contract AF 30(602)-2575, "Centipede TWT," Microwave Laboratory Report No. 1116, Stanford University (October 1963).
6. Quarterly Status Report No. 11 for Contract AF 30(602)-2575, Microwave Laboratory Report No. 1224, Stanford University (September 1964).

## PART II: PHASE-SHIFTER AND DELAY-LINE MECHANISMS

### III. TRANSVERSE-WAVE STUDIES

(T. Wessel-Berg, \* B. Hoeks)

In this final report we present a summary and conclusions of our investigation. The complete report will be forthcoming soon.

#### A. OBJECTIVE

The objective of this project is to study a possible approach to broadband high-powered amplifiers which involves interaction between an electron beam and a circuit in the presence of an axial dc magnetic field. This amplification mechanism depends on interaction between the transverse motion of the beam with transverse electric fields. Examples of such interaction are the Adler low-noise quadrupole amplifier, and the so-called fast-wave tubes where a rotating electron beam is interacting with an ordinary fast electromagnetic wave in a smooth waveguide. In the first case this type of interaction was used for low-noise amplifiers; in the second case, for very high frequency amplifiers. There are many possible variations of this kind of interaction, however, which would be appropriate to any frequency range and not merely for low noise.

The analysis of transverse-wave propagation in accelerated electron streams has been completed with the issuance of a technical report (and dissertation) "Space charge waves in an accelerated parallel-flow electron beam in a constant magnetic field," by Bas Hoeks, Microwave Laboratory Report No. 1205, July 1964.

The main results of the investigation are summarized in the following sections of this report .

In the coming year the emphasis will be shifted to transverse wave interaction in a crossed field beam rather than a drifting beam. The

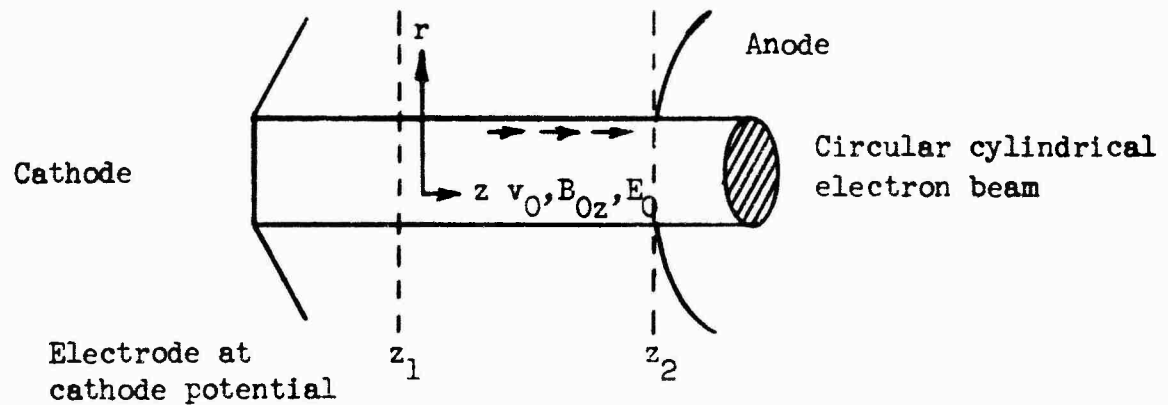
---

\* Project supervisor

shift of objectives towards crossed field interaction is motivated by possible applications in time and phase delay devices.

## B. INTRODUCTION

Consider a parallel-flow Pierce electron gun as shown in the figure. For this type of gun the electrodes are shaped in such a way that the unperturbed electric forces acting on the electrons are in the axial (z-) direction only.



Pierce electron gun.

The equation describing the drift velocity  $v_0(z)$  is therefore essentially that of a parallel-plane space-charge-limited diode, namely

$$v_0(z) = \frac{dz}{d\tau} = 3 \left( \frac{\eta J_0}{6\epsilon_0} \right)^{1/3} z^{2/3} = \left( \frac{\eta J_0}{2\epsilon_0} \right) \tau^2, \quad (1)$$

where

$$\eta = e^0 / r^0$$

$$e^0 = \text{negative electron charge}$$

$$m^0 = \text{electron rest mass}$$

$$J_0 = \rho_0(z) v_0(z) = \text{dc beam current} = \text{constant}$$

$$\rho_0 = \text{dc space charge density}$$

$$\epsilon_0 = \text{permittivity in vacuum}$$

$$\tau = \text{dc electron transit time} .$$

In addition to the applied axial electric field  $E_0$ , there is also an applied axial magnetic field  $B_{0z}$  and a circular magnetic field  $B_{0\theta}$  due to the beam current. Inside the beam,  $B_{0\theta}$  is given by

$$B_{0\theta} = \frac{1}{2} \mu_0 J_0 r , \quad r \leq b , \quad (2)$$

as  $J_0$  is not a function of  $r$  or  $z$ .

where

$$\mu_0 = \text{permeability in vacuum}$$

$$r = \text{radius}$$

$$b = \text{beam radius} .$$

We have considered only the nonrelativistic case primarily for three reasons: (a) no closed expression could be found for  $v_0(z)$  in the relativistic case; (b) the effect of  $B_{0\theta}$  upon the parallel dc electron flow can be neglected; and (c)  $B_{0\theta}$  can be taken small as compared to finite values of  $B_{0z}$  and can therefore be neglected in the ac force equations to be given later. The result is that  $r, \theta, z$ -dependent product solutions can then be readily separated from these equations.

Referring again to the figure, we wish to establish whether the small-perturbed noise fluctuations coming off the cathode will grow or decay as a function of the axial distance  $z$ , and furthermore what effect the axially applied dc magnetic field  $B_{Oz}$  has upon these fluctuations. We shall consider the solutions between the planes  $z_1$  and  $z_2$  only, where  $z_1$  lies just beyond the potential minimum of the beam.

In this analysis Maxwell's equations are linearized and the Eulerian description of the force equations is utilized. It is assumed that (a) the velocity of any point is single-valued, (b) no electron collisions occur, (c) the fields due to the image charges on the beam electrodes can be neglected, and (d) the beam is infinitely long, i.e., the solutions derived for this case will approach the correct values if the beam diameter is small compared to its finite length.

### C. THE BEAM EQUATIONS

The linearized ac beam equations are given by (rationalized MKS units)

$$\left. \begin{aligned} \nabla \times \vec{E} + \frac{\partial \vec{B}}{\partial t} &= 0 \\ \nabla \times \vec{B} - \frac{1}{c^2} \frac{\partial \vec{E}}{\partial t} &= \mu_0 \vec{J} \\ \nabla \cdot \vec{E} &= \rho / \epsilon_0 \end{aligned} \right\} \quad (3)$$

$$\left. \begin{aligned} \nabla \cdot \vec{J} + \frac{\partial \rho}{\partial t} &= 0 ; \quad \vec{J} = \rho_0 \vec{v} + \rho \vec{v}_0 ; \quad \eta = e^0 / m^0 \\ \left( \frac{\partial}{\partial t} + \vec{v}_0 \cdot \nabla \right) \vec{v} + \left( \vec{v} \cdot \nabla \right) \vec{v}_0 + \eta \vec{B}_{Oz} \times \vec{v} &= \eta (\vec{E} + \vec{v}_0 \times \vec{B}) \end{aligned} \right\} \quad (4)$$

and

$$v_r(b, \theta, z, t) = \left( \frac{\partial}{\partial t} + \vec{v}_0 \cdot \nabla \right) s_r(b, \theta, z, t) \quad , \quad (5)$$

where  $v_r$  and  $s_r$  are the radial velocity and displacement, respectively.

If  $\vec{E}^+(b, \theta, z, t)$  and  $\vec{E}^-(b, \theta, z, t)$  signify electric field intensities just outside and inside the beam, respectively, then the boundary conditions at the beam radius  $b$  are found to be given by

$$\left. \begin{aligned} \vec{a}_r \cdot (\vec{B}^+ - \vec{B}^-) &= 0 & \vec{a}_r \times (\vec{B}^+ - \vec{B}^-) &= \mu_0 \vec{a}_z J_0 s_r \\ \vec{a}_r \times (\vec{E}^+ - \vec{E}^-) &= 0 & \vec{a}_r \cdot (\vec{E}^+ - \vec{E}^-) &= \rho_0 s_r / \epsilon_0 \end{aligned} \right\} \quad , \quad (6)$$

where  $\vec{a}_r$  and  $\vec{a}_z$  are radial and axial unit vectors, respectively.

It can be shown that four of the six boundary Eqs. (6) are independent.

The problem can now be approached in two ways:

1. One can solve the homogeneous system [Eqs. (3)-(5)] inside the beam and Maxwell's equations in free space and match these solutions at the beam boundary by means of Eq. (6). Unfortunately, this method leads to difficulties. After separating the variables  $r, \theta, t$  from Eqs. (3)-(5) there remain ten simultaneous first-order differential equations with the variable coefficients  $\rho_0(z)$  and  $v_0(z)$ . We have considered various ways of reducing the order of this system by means of the following methods:

- (a) Quasi-static approximations
- (b) Transformation of the beam equations to a frame of reference that moves along the  $z$ -axis at the dc beam speed  $v_0(z)$ .
- (c) Thin beam approximations.

It was found that only the quasi-static approximation was useful. The system order could then be reduced from ten to eight. Although we have obtained first-order WKB solutions of this system, it did not appear feasible to match these solutions to the free space solutions at the beam boundary.

2. A comparatively simpler method is the utilization of retarded potentials, because it permits us to make effective use of thin beam approximations in order to reduce the order of the system. We introduce

$$\vec{E} = -\nabla\phi - \frac{\partial\vec{A}}{\partial t} ; \vec{B} = \nabla \times \vec{A} \quad (7)$$

in Eq. (3), where  $\phi$  and  $\vec{A}$  are retarded scalar and vector potentials, respectively, and the gauge is given by

$$\nabla \cdot \vec{A} + \frac{1}{c^2} \frac{\partial\phi}{\partial t} = 0 \quad (8)$$

Then Eqs. (3) become

$$\left. \begin{aligned} \nabla^2\phi - \frac{1}{c^2} \frac{\partial^2\phi}{\partial t^2} &= -\rho/\epsilon_0 \\ \nabla^2\vec{A} - \frac{1}{c^2} \frac{\partial^2\vec{A}}{\partial t^2} &= -\mu_0 \vec{J} \end{aligned} \right\} , \quad (9)$$

of which the first-order solutions are given by

$$\phi(r,\theta,z,t) = \frac{1}{4\pi\epsilon_0} \int_V \frac{\rho\left(t - \frac{R}{c}\right)}{R} dV + \frac{1}{4\pi\epsilon_0} \int_S \frac{\rho_0 s_r\left(t - \frac{R}{c}\right)}{R} dS , \quad (10)$$

and

$$\vec{A}(r, \theta, z, t) = \frac{\mu_0}{4\pi} \int_V \frac{\vec{J}\left(t - \frac{R}{c}\right)}{R} dV + \frac{\mu_0}{4\pi} \int_S \frac{\rho_0 \vec{v}_0 s_r\left(t - \frac{R}{c}\right)}{R} dS, \quad (11)$$

where

$$R^2 = (z - z_1)^2 + r^2 + r_1^2 - 2rr_1 \cos(\theta - \theta_1)$$

$r, \theta, z$  = coordinates of the observation point

$r_1, \theta_1, z_1$  = variables of integration

$V$  = volume of the beam

$S$  = surface of the beam

$s_r$  = radial ac displacement

$v_0$  = dc beam velocity

$\rho_0$  = dc charge density .

Although (10) and (11) satisfy (9), the gauge (8) requires in addition that we have

$$\nabla \cdot \vec{J} + \frac{\partial \rho}{\partial t} = 0 ; J_0 (\nabla \cdot s_r) + \frac{\partial}{\partial t} (\rho_0 s_r) = \rho_0 v_r . \quad (12)$$

Thus, by assuming a current density distribution  $\vec{J}$  inside the beam, the distributions of the remaining quantities can be determined from (12).

We now have obtained an integro-differential system consisting of Eqs. (4), (5), (7), (10) and (11). Although still difficult to solve in general, we will see below that the introduction of thin beam approximations allows us to solve the problem.

The integrals (10) and (11) could be partially integrated for a thick beam by (a) taking the Fourier transforms with respect to  $z$  and  $t$  of the variables of the integrands, (b) assuming  $r, \theta$ -variations in accordance with the solutions of Bessel's equation, and (c) assuming an infinitely long beam.

If we now let the radius  $r$  as well as the beam radius  $b$  approach zero in (10) and (11), it is found that the volume integrals become vanishingly small as compared to the surface integrals. The explicit expressions for  $\phi$  and  $\vec{A}$  inside a very thin beam are then given by

$$\left. \begin{aligned} \phi &= \frac{\rho_0(z)}{2\epsilon_0} e^{j\omega t} \sum_{m=1}^{\infty} r^m \left[ e^{jm\theta} \hat{s}_{-m}(z) + e^{-jm\theta} \hat{s}_{+m}(z) \right] \\ A_{\pm} &\approx 0 \\ A_z &= \frac{\mu_0 \rho_0 v_0}{2} e^{j\omega t} \sum_{m=1}^{\infty} r^m \left[ e^{jm\theta} \hat{s}_{-m}(z) + e^{-jm\theta} \hat{s}_{+m}(z) \right] \end{aligned} \right\}, \quad (13)$$

where we have utilized the circularly polarized variables

$$\begin{aligned} A_{\pm}(r, \theta, z, t) &= A_r \pm jA_{\theta} \\ \hat{s}_{\pm m}(z) &= \hat{s}_{rm} + j \hat{s}_{\theta m} \end{aligned} \quad (14)$$

We observe in (13) that all integrations occurring in (10) and (11) could be performed. However, this can only be done for  $m \geq 1$ , and not for  $m = 0$ . In what follows we shall therefore consider only the values of  $m$  which are equal to or greater than unity.

#### D. THIN BEAM SOLUTIONS

Upon utilizing Eqs. (4), (7), and (13) we arrive at the two second-order differential systems

$$\left. \begin{aligned} \left( j\omega + v_0 \frac{d}{dz} \right) \hat{s}_{\pm m} &= \hat{v}_{\pm m} \\ \left( j(\omega \pm \omega_c) + v_0 \frac{d}{dz} \right) \hat{v}_{\pm m} &= -\frac{1}{2} \omega_p^2 \left( 1 - \frac{v_0^2}{c^2} \right) \hat{s}_{\pm m} \end{aligned} \right\}, \quad (15)$$

where

$\hat{s}_{\pm m}(z)$  = pos./neg. circularly polarized ac displacement

$\hat{v}_{\pm m}(z)$  = pos./neg. circularly polarized ac velocity

$v_0(z)$  = dc beam velocity

$\omega_p(z) = [\eta \rho_0(z) / \epsilon_0]^{1/2}$  = angular plasma frequency

$\omega_c = \eta B_{0z}$  = angular cyclotron frequency

$\omega$  = angular signal frequency

$\eta = e^0 / m^0$

$e^0$  = negative electron charge

$m^0$  = electron rest mass

$\rho_0(z)$  = dc space charge density

$\epsilon_0$  = permittivity in vacuum

$c$  = speed of light in vacuum

$m$  = circular mode number equal to or greater than unity.

In what follows we shall briefly describe some of the methods which we have utilized to solve (15). A detailed description can be found in our forthcoming report.

Since the coefficients of (15) are independent of  $m$  and the non-relativistic case is considered, the subscript  $m$  as well as the term  $v_0^2/c^2$  (representing the  $\vec{v}_0 \times \vec{B}$  term) will be dropped. Furthermore, since the two differential systems are identical except for a change of sign of  $\omega_c$ , it suffices to consider the negatively polarized solutions only. Thus, the set of equations to be solved is

$$\left. \begin{aligned} \left( j\omega + v_0 \frac{d}{dz} \right) \hat{s}_- &= \hat{v}_- \\ \left[ j(\omega - \omega_c) + v_0 \frac{d}{dz} \right] \hat{v}_- &= -\frac{1}{2} \omega_p^2 \hat{s}_- \end{aligned} \right\} \quad (16)$$

In order to facilitate the solution of (16) we introduce the dc electron transit time  $\tau$  as defined by (1), so that we obtain

$$\frac{1}{2} \omega_p^2 = \frac{\eta \rho_0}{2\epsilon_0} = \frac{\eta J_0}{2\epsilon_0} \left/ \left( \frac{\eta J_0 \tau^2}{2\epsilon_0} \right) \right. = 1/\tau^2 \quad (17)$$

By further putting

$$\left. \begin{aligned} X &= \omega\tau \quad ; \quad p = \omega_c/(2\omega) \\ \hat{s}_- &= a_1(X) e^{-jX} \quad ; \quad \hat{v}_- = \omega a_2(X) e^{-jX} \end{aligned} \right\} \quad (18)$$

Eqs. (16) become in matrix notation

$$\frac{d\tilde{a}}{dX} = \tilde{A}(X)\tilde{a} \quad , \quad (19)$$

where

$$\tilde{a} = \begin{pmatrix} a_1 \\ a_2 \end{pmatrix} \quad , \quad \text{and} \quad \tilde{A} = \begin{pmatrix} 0 & 1 \\ -1/X^2 & 2jp \end{pmatrix} \quad .$$

It will be assumed that  $\omega$  , and hence  $X$  and  $p$  , are real. Now, it is well known that if  $\tilde{A}$  is independent of  $X$  , one can introduce a matrix  $\tilde{P}$  such that

$$\begin{aligned} \tilde{a} &= \tilde{P}\tilde{C} \quad , \\ \frac{d\tilde{C}}{dX} &= \tilde{P}^{-1}\tilde{A}\tilde{P}\tilde{C} \quad , \end{aligned} \quad (20)$$

and

$$\tilde{P}^{-1}\tilde{A}\tilde{P}$$

is diagonal. The solutions  $\tilde{C}$  are then called normal mode solutions since they characterize the behavior of the system. If, however,  $\tilde{A}$  is a function of  $X$  , we found that, although  $\tilde{A}$  still can be diagonalized, the solutions  $\tilde{C}$  no longer characterize the system, since  $\tilde{P}(X)$  is then generally a series containing information with regard to both amplitude and phase. We have therefore attempted to find solutions together with their regions of validity such that the transformation

matrix  $\tilde{P}(X)$  is approximately a constant. The solutions  $\tilde{C}$  then represent fairly good normal mode solutions.

The diagonalization of  $\tilde{A}(X)$  has been accomplished by means of first-order WKB solutions as well as by asymptotic series for either small or large values of

$$pX = \frac{1}{2} \omega_c \tau = \frac{1}{2} \omega_c \left( \frac{\sigma \epsilon_0}{\eta J_0} \right)^{1/3} z^{1/3}, \quad (21)$$

where  $z$  is the axial distance from the potential minimum at the cathode. Since it follows from (17) that  $\omega_p$  is singular at this potential minimum, it is evident that the solutions for small values of  $|pX|$  are not valid at  $\tau = 0$ ,  $z = 0$ , or  $X = 0$ . They are, however, valid for  $p = 0$  or  $\omega_c = 0$ . We now proceed to discuss the behavior of the transverse displacement  $\hat{s}_-$ , and the transverse and axial electric field intensities  $\hat{E}_-$  and  $\hat{E}_z$ , respectively. For the sake of brevity we include the following two cases only

Case I,  $\omega_c = 0$  ;  $\omega_p \neq 0$

In this case the solutions are exact, namely

$$\hat{s}_- = \tau^{1/2} \left[ c_{0+} e^{1/2j\sqrt{3}\ln(\omega\tau)} + c_{0-} e^{-1/2j\sqrt{3}\ln(\omega\tau)} \right] e^{-j\omega\tau}, \quad (22)$$

where  $c_{0\pm}$  are constants and  $\tau(z)$  is given by

$$\tau = \left( \frac{\sigma \epsilon_0}{\eta J_0} \right)^{1/3} z^{1/3}. \quad (23)$$

The electric field intensities are found to be

$$\left. \begin{aligned} \hat{E}_-(z) &= - \frac{\omega_p^2(z)}{2\eta} \hat{s}_-(z) \\ \hat{E}_z(z) &= - \left( \frac{d}{dz} + \frac{j\omega v_0}{c^2} \right) \left( \frac{\omega_p^2}{2\eta} \hat{s}_- \right) \end{aligned} \right\} . \quad (24)$$

By considering (17), (22), (23) and (24) one observes that as  $\tau$  or  $z$  increases (a)  $\hat{s}_-$  grows, (b)  $\hat{E}_-$  decays, (c) the term of  $\hat{E}_z$  involving  $(d/dz)$  decays, and (d) the term of  $\hat{E}_z$  involving  $1/c^2$  grows.

Case II,  $\omega_c \neq 0$  ;  $\omega_p \neq 0$

In this case the first-order WKB solution for large  $|pX|$  is given by

$$\hat{s}_- = f^{-1/2} [c_{0+} e^{j\alpha} + c_{0-} e^{-j\alpha}] e^{j(p-1)X} , \quad (25)$$

where  $c_{0\pm}$  are constants and we have

$$f^2 = p^2 + \frac{1}{X^2}$$

$$\alpha = \sqrt{1 + (pX)^2} - \ln \left[ \frac{1 + \sqrt{1 + (pX)^2}}{pX} \right]$$

$$p = \omega_c / (2\omega)$$

$$X = \omega\tau .$$

We observe from Eq. (25) that as  $X \tau$  or  $z$  increases, the magnitude of  $\hat{s}_-$  will at first grow in a fashion similar to that of (22), but will then approach an asymptotic value beyond a certain distance from the cathode. The larger the value of  $\omega_c$ , the shorter this distance will be. In view of this we believe that the minimum value of  $\omega_c$  (and hence the axially applied dc magnetic field) should be such that the asymptotic value of  $\hat{s}_-$  is reached just before the beam leaves the electron gun. This will be approximately the case when

$$|pX| \geq 3 \quad ,$$

or, in view of (21), when

$$B_{0z} \geq 5.1 (J_0/L)^{1/3} \quad , \quad (26)$$

where

$B_{0z}$  (gauss) = axial dc magnetic flux density,

$J_0$  (amp./sq. Meter) = dc beam current density, and

$L$  (meter) = distance between cathode and beam exit.

Except for the term of  $\hat{E}_z$  involving  $1/c^2$  which behaves as  $\hat{s}_-$  does, the electric field intensities will also decay in this case as a function of  $z$ .

Finally, the effect of  $\Theta$ -variations can be studied by considering the ratios of the  $m$ -th components of the electric field intensities and

the transverse displacement, namely

$$\frac{E_{-m}(r, \theta, z, t)}{s_{-m}(r, \theta, z, t)} = - \frac{\omega_p^2}{2\eta}$$

$$\frac{E_{zm}(r, \theta, z, t)}{s_{-m}(r, \theta, z, t)} = - \frac{r}{4m} \cdot \frac{\left( \frac{d}{dz} + \frac{j\omega v_0}{c^2} \right) \left( \omega_p^2 \hat{s}_{-m} \right)}{\hat{s}_{-m}(z)} \quad (27)$$

One observes that for a given magnitude of  $s_{-m}(r, \theta, z, t)$ ,  $E_{zm}(r, \theta, z, t)$  approaches zero as  $m \rightarrow \infty$  or  $r \rightarrow 0$  and that  $E_{-m}$  is not affected this way. This phenomenon indicates that we are primarily dealing with a transverse wave interaction.

#### E. CONCLUSIONS

In conclusion we wish to mention that (1) we succeeded in studying the purely transverse wave interaction in an accelerated electron beam by utilizing the retarded potential method and by introducing thin beam approximations, and that (2) the application of an axial dc magnetic field reduces the noise fluctuations at the beam exit plane. In addition, we wish to mention that several authors have shown by means of a one-dimensional analysis that purely axially directed noise fluctuations will generally decay on an accelerated beam. In this case, an axially directed magnetic field would, of course, have no effect.

Although we have not succeeded in studying the effects of interaction between transverse and axial waves, we have shown that the application of an axial magnetic field will generally have a favorable effect on the noise reduction.

#### IV. WHISTLER MODE PROPAGATION IN SOLIDS

(G. S. Kino,\* J. Eidson)

##### A. OBJECTIVE

The purpose of this study is to investigate wave propagation through solid-state material which depends on plasma effects resulting from the collective motion of the conduction electrons. In particular, the so-called helicon or whistler mode of propagation is of great interest because the loss per wavelength of this mode is determined by the ratio of the cyclotron frequency to the collision frequency, rather than by the ratio of the working frequency to the collision frequency. Consequently, because high cyclotron frequencies are relatively easy to obtain, the loss in these modes can be small. The modes themselves are intrinsically interesting because (1) they are extremely slow waves with wave velocities a small fraction of the velocity of light, (2) there is the possibility of using nonuniform static magnetic fields to cause refractive focusing of these waves; by changing the magnetic fields, both the phase delay and the point in the semiconductor where the field is a maximum may be altered. This has obvious applications to microwave switching and delay line problems. There is also the possibility that when dc electric fields are applied to the semiconductor there will be interactions between electrons and holes which can give rise to amplification or instabilities. It is intended that most of our work will be carried out using semiconductors rather than metals. In a metal, helicon mode propagation is normally observed at very low frequencies in the kilocycle range. With a semiconductor material such as indium antimonide, characterized by a high plasma frequency of perhaps 700 kMc and a fairly high collision frequency of  $\approx 30$  kMc at  $77^{\circ}\text{K}$ , the best operating frequency is typically in the millimeter wave range. Large cyclotron frequencies are easily obtainable due to the very small effective mass of the electrons

---

\* Project Supervisor

in such semiconductors. In indium antimonide, for instance, the effective mass of the electron is  $1/70$  of that of a free electron.

The early phase of the study will be to repeat a measurement of helicon wave propagation through indium antimonide of the same type carried out by a number of workers elsewhere. This is being done in order to gain experience with this type of experiment before proceeding to further more sophisticated studies.

#### B. PRESENT STATUS

This project has been active for only one quarter. During this quarter we have made preliminary calculations on the propagation of whistler modes in InSb . Samples have been obtained with collision frequencies of about 30 kMc.

An initial experiment to measure the transmission through a sample is being constructed. This work will be done at about 55 kMc and a source at this frequency is being assembled and tested for use on this and a related project.

## V. CARRIER WAVE PROPAGATION IN SEMICONDUCTORS (GUNN OSCILLATIONS)

(G. S. Kino,\* J. Owens)

### A. OBJECTIVE

The purpose of this study is to investigate Gunn oscillations<sup>1</sup> in semiconductors. This is a type of oscillation first observed by Gunn when he applied large electric fields to gallium arsenide and indium phosphide. Typically, with gallium arsenide, in which the most reproducible results have been obtained using  $n^+n$  contacts of tin and highly doped n-type gallium arsenide, he observed microwave oscillations when the applied field was of the order of 1300 volts per cm. The oscillation frequency is approximately the reciprocal of the transit time of the electron from one end of the semiconductor to the other. Coherent oscillations were obtained only with very short samples of semiconductors corresponding to oscillation frequencies of the order of 1,000 megacycles or more. The experiment has been repeated in many laboratories. The device should obviously provide an important new source of microwave power because of its simplicity and ultimate cheapness in manufacture.

Our purpose is to investigate the source of these oscillations and to determine a mechanism for their generation. It is our belief, shared by all working in the field, that they are due to a volume effect, not a junction effect, in the semiconductor. We believe the oscillations are associated with a wave propagating through the semiconductor at the drift velocity of the electrons, which is approximately  $10^7$  cm/sec in GaAs. This concept is closely related to others which refer to a domain of charge moving through the semiconductor at the drift velocity, or to a shock wave moving through the semiconductor. Sufficient experiments have been done by Gunn to prove the point that there is indeed a region of excess electron charge followed by a region of electron charge deficiency moving through the semiconductor at the electron drift velocity.

---

\* Project Supervisor

We believe that such volume effects are of utmost importance and may point to new ways of obtaining waves which can propagate through a semiconductor at the electron drift velocity with very little loss or, indeed, with growth. Already it has been noted that interactions between electrons and sound waves in semiconductors can be observed.<sup>2,3,4</sup> It is therefore our intention to try and understand how oscillations are generated, how waves may be propagated through the volume of the semiconductor, how their phase velocity and phase delay may be controlled, and the conditions for instability or growth of such waves. In particular, with the use of injecting contacts it may be possible to inject a pulse of charge at one end of a semiconductor and observe its time of travel through the semiconductor. The fields associated with this pulse of charge then would constitute a wave propagating through the semiconductor at a velocity comparable to the electron drift velocity. The semiconductor itself, therefore, may behave very like a transmission line with a very slow velocity of propagation under these conditions.

#### B. THEORETICAL WORK

A great deal of theoretical work on the subject has been undertaken with the cooperation of C. F. Quate and T. Wessel-Berg, who are carrying out similar studies on other contracts. The properties of the waves which can propagate on drifting carriers of a semiconductor have been investigated in some detail using the methods given in a paper by Quate.<sup>4</sup> The small signal theory has been extended to take account of the situation when the electron drift velocity is saturated because of interaction with optical phonons. Under these conditions, the presence of an rf field makes no difference to the velocity of the electrons. Consequently, there is no ac velocity. An initial increment of charge leaving the cathode end of the system can thus pass along the semiconductor unchanged in form, provided diffusion effects are negligible. Using this approach it is possible to show that a semiconductor diode should, like the Lwellyn diode, have a negative resistance when the transit time of the electrons through it is approximately  $2\pi$  radians. However, the negative

resistance is not sufficient to account for the experimental results obtained with the Gunn diode. A further mechanism is needed. Mechanisms associated with intervalley scattering and with space charge instabilities of various kinds are currently being investigated.

### C. EXPERIMENTAL WORK

The object of this project is to study and to attempt to explain the Gunn effect, a current instability at high current densities in III-V semiconductors such as GaAs.

Samples of GaAs have been obtained and cut into thin, 1 cm-long samples and ohmic contacts alloyed onto the ends of the samples. At high fields, incoherent oscillations have been observed. At fields near the threshold of the instability, seemingly coherent pulses of noise have been seen. It is hoped that coherent oscillations can be sustained in long samples. In this case, observation can be made on the longitudinal variation of rf field and current along a sample without the problems associated with such measurements in short samples.

Some trouble has been encountered in maintaining consistency of ohmic contact. The contact resistance seems to increase with time. At present, experiments are being conducted with different alloys and alloying methods to alleviate this problem.

#### REFERENCES FOR PART V

1. J. B. Gunn, "Instabilities of current in III-V semiconductors," I.B.M. Journal, 141-159 (April 1964).
2. D. L. White, "Amplification of ultrasonic waves in piezoelectric semiconductors," J. Appl. Phys. 33, 2547 (1962).
3. A. R. Hutson, J. H. McFee and D. L. White, "Ultrasonic amplification in CdS," Phys. Rev. Letters 7, No. 6 237 (September 15, 1961).
4. K. Bløtekjaer and C. F. Quate, "The coupled modes of acoustic waves and drifting carriers in piezoelectric crystals," Proc. IEEE 52, 4, 360-377 (April 1964).

## VI. ACOUSTIC WAVE DEVICES

(H. J. Shaw,\* D. K. Winslow, E. Lean)

### A. INTRODUCTION

A very important approach to the realization of variable time delay and phase shift at microwave frequencies is through the use of microwave acoustic waves in solids. In all such devices and applications of acoustic waves at present, one of the largest practical difficulties lies in the coupling loss in transducers designed to couple microwave electromagnetic energy into microwave acoustic waves. In the present program we have recently begun setting up facilities for the fabrication of new types of transducers, particularly employing thin film techniques. The objective here is to fabricate working models of new approaches to transducer design, and to test these designs in the laboratory by measurements of coupling efficiency and passband characteristics. At this time it appears that the proper use of thin films may lead to transducers of very low conversion loss.

### B. PRESENT STATUS

A number of thin films have been evaporated in this laboratory in the past for a variety of purposes and, to date on this contract, equipment has been modified and acquired to evaporate films for our purpose here and to measure the coupling efficiency of these transducers. A typical nickel film transducer with a rutile rf dielectric resonator and delay line for operation at S-band is shown in Fig. 1.

The method of coupling the rf magnetic field to the nickel film used here was developed on another contract in this laboratory. The rutile dielectric resonator increases the rf magnetic field for a given power

---

\* Project Supervisor

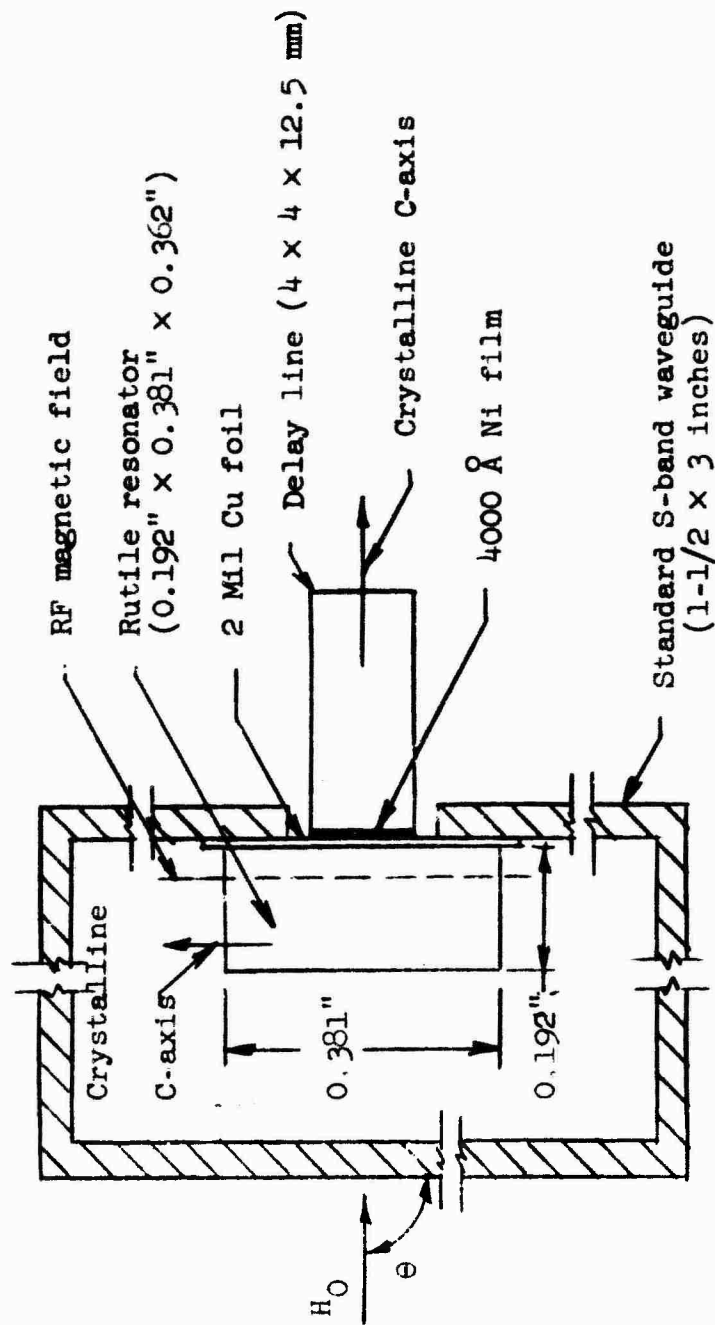


FIG. 1--Resonator and delay line (not to scale).

input by a factor of 25 to 30, compared to the magnetic field of a metal resonator of similar shape. Here, as in the previous experiments, the coupling efficiency is determined by observing the amplitudes of the incident and reflected rf pulses. An incident pulse of 1 mW of rf power at 3000 Mc, for example, of one microsecond duration is applied to the resonator. This pulse is converted to an acoustic wave by the magnetostrictive nickel film transducer attached to one end of the low loss dielectric delay line. The acoustic wave propagates in the delay line, reflects from the end, and is returned to the nickel film transducer, where the acoustic pulse is converted to rf, which is observed as an echo. For a single crystal sapphire rod 2 cm in length, the delay time between the initial exciting pulse and the first echo is about four microseconds. A number of echoes are usually observed as the magnetostrictive transducer couples out a fraction of the acoustic energy after each round trip in the delay line. The velocity of the acoustic wave is obtained from a determination of the time between successive pulses and the acoustic attenuation by a measurement of the amplitudes of successive pulses. The conversion efficiency, a measure of how efficiently a transducer converts rf energy to acoustic energy, is obtained by measuring the difference in amplitudes of the initial exciting rf pulse and the first echo. This difference includes the transducer efficiency twice, from rf to acoustic power and on the return from acoustic to rf power, and the acoustic attenuation in the delay line. For the conversion efficiency as given in this report, the acoustic attenuation of the delay line is subtracted from the difference in amplitude of the initial pulse and the first echo, and the result is divided by two, which gives the one-way conversion efficiency. Typical values for this conversion efficiency for nickel films measured in this laboratory are about 30 dB for both longitudinal and shear waves. For comparison, thin quartz wafers 0.005 in. thick, bonded to the delay line and used in this laboratory on other contracts, have a conversion efficiency of about 20 dB. Recently, a zinc oxide wafer similar to the quartz gave a conversion efficiency of 11 dB. The zinc oxide wafer represents the best conversion efficiency obtained to date. Recently, cadmium sulfide evaporated films have been reported to have given a conversion efficiency of approximately

10 dB. This work was done in another laboratory.<sup>1</sup> These piezoelectric films show great promise and are discussed in more detail below.

Single-layer nickel films have been evaporated on different substrates and typical results are summarized in Table I. The arrangement of apparatus in the vacuum bell jar is shown in Fig. 2. Note that a cold trap in the bell jar is used in all cases. Early experiments showed this gave considerable improvement on the conversion efficiency of the nickel films evaporated under these conditions. The substrate temperature is important, as can be seen from Table I. The temperature given here is the temperature given by a thermocouple in the substrate holder. The substrates (acoustic delay lines) here were sapphire and rutile approximately  $6 \times 6 \times 20$  mm. As shown in Table I, the conversion efficiencies for the best nickel films were 30 dB for shear waves in rutile (sample 9) and 31 dB for longitudinal waves in sapphire (sample 4) at the S-band frequencies as given.

Equipment is now being designed and assembled for the evaporation of multilayer films. The purpose here is to determine the effect on the conversion efficiency of a number of half-wavelength layers of thin film transducer materials separated by half-wavelength inactive material. The first experiment will consist of two layers of nickel film separated by a half-wavelength film of magnesium fluoride. With this equipment we can also evaporate a number of quarter wavelength layers which will act as an impedance transformer between the transducer and the delay line. Also, with this multi-source arrangement, four different materials can be evaporated during a single run. This allows a sufficient number of films for both the multilayer transducer and the impedance transformer, so that the complete system can be evaporated without removing the work from the vacuum.

Cadmium sulfide (CdS) one-half acoustic wavelength in thickness shows considerable promise as an efficient transducer, as stated above.<sup>1</sup> There are several methods which have been used under a variety of conditions.<sup>1,2,3</sup> These films have been successfully evaporated with the preferred orientation, the C-axis of hexagonal CdS normal to the film surface, for the generation of longitudinal acoustic waves.<sup>2,3</sup> These methods use either the co-evaporation of cadmium and sulfur or the

TABLE I  
 Summary of Results Showing the Conversion Efficiency of  
 Deposited Nickel Films under Different Conditions

Substrate	Sapphire 4	Sapphire 3	Sapphire 8	Sapphire 5	Sapphire 8	Rutile 9	Rutile 8
Freq.	2720	2580	2700	2700	2700	2500	2700
$Q_L$ (Loaded Q of Microwave Cavity)	500	~500	500	700	600	~500	600
Conversion	31 dB	> 50 dB	> 50 dB	> 50 dB	40 dB		
Efficiency	39 dB	> 50 dB	> 50 dB		35 dB	30 dB	35 d
Velocities	$11.35 \times 10^5$ cm/sec	"	"			$5.5 \times 10^5$ cm/sec	
Attenuation	~7 dB/cm					2 dB/cm	2.5 dB/
Mag. Field Kilogauss	6.1	5.1	4.8	6.4	6.1	5.85	4.9
Power input (peak)	50 watts	75 watts	200 watts	200 watts		10 mW	10 mW
Nickel film thickness	3800 A	3300 A				3200 A	
Substrate temp.	300° C	400° C	500° C	200° C	300° C	200° C	100° C
Pressure	$2 \times 10^{-6}$ Torr	$2 \times 10^{-6}$ Torr	$2 \times 10^{-6}$ Torr	$1 \times 10^{-6}$ Torr	$1 \times 10^{-6}$ Torr	$1 \times 10^{-6}$ Torr	$1 \times 10^{-6}$ Torr

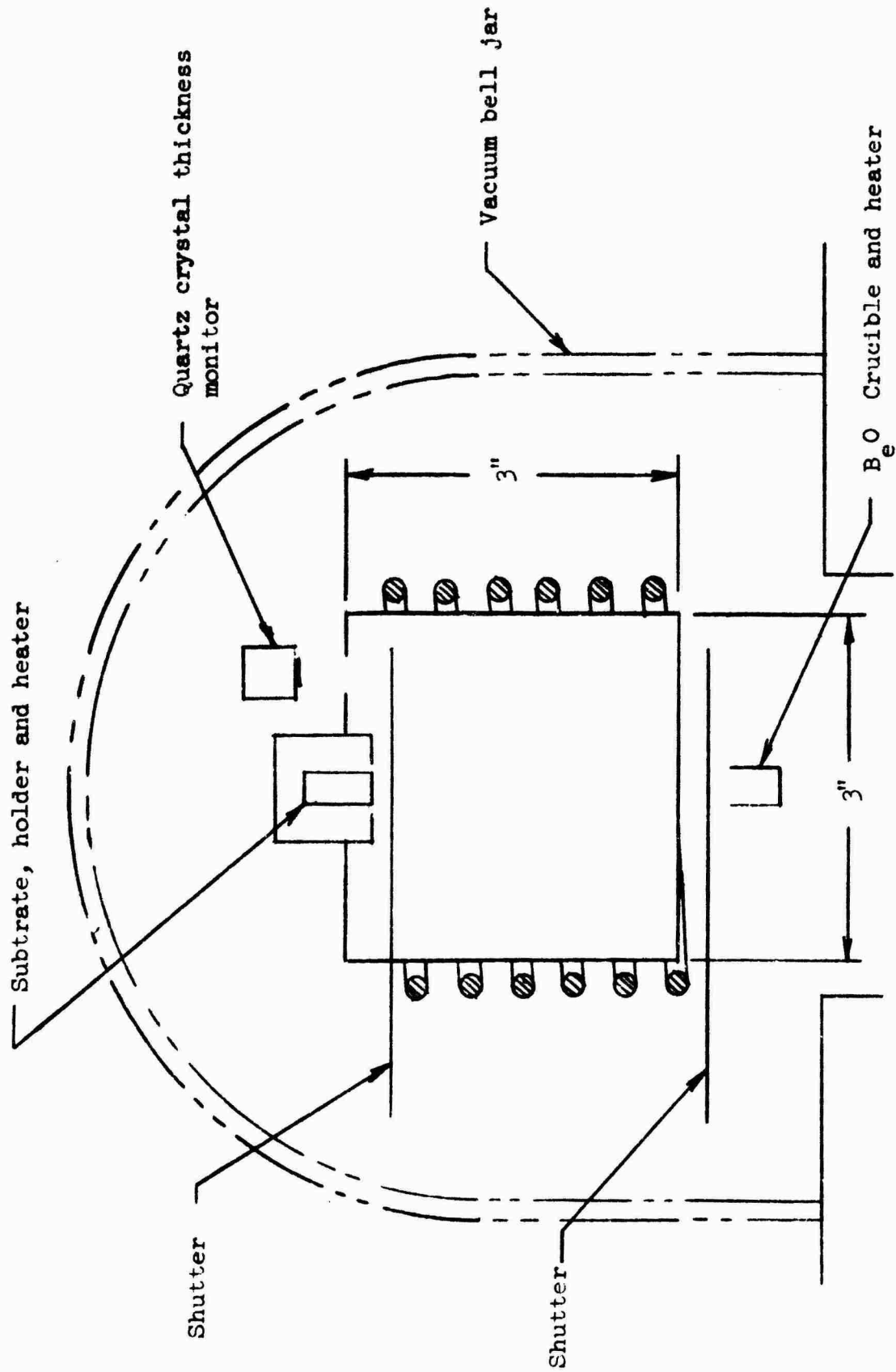


FIG. 2--Schematic diagram of apparatus for the vacuum deposition of nickel films on single crystal sapphire and rutile.

co-evaporation of CdS and sulfur. By controlling the direction of the evaporation beam, i.e., at  $35^{\circ}$  to  $40^{\circ}$  with the substrate, the hexagonal CdS can be properly oriented for the generation of transverse waves.<sup>1</sup> An evaporating station has been equipped for the simultaneous evaporation of cadmium and sulfur, and a number of preliminary runs have been made. These films are between one and two microns thick. Procedures and methods for controlling and monitoring thickness, source temperatures, substrate temperature, etc. are underway. Equipment and procedures for the rf evaluation of these films is also proceeding. Procedures are also being developed to evaporate multilayer active CdS films in the near future. The method here will be to evaporate layers of CdS, each one-half wavelength thick. Alternating layers will be active hexagonal CdS films, with the layers between composed of non-piezoelectric cubic CdS.

#### REFERENCES

1. N. F. Foster, "Cadmium Sulfide Evaporated Layer Transducer," Symposium on Sonics and Ultrasonics, IEEE, Oct. 14-16, 1964. Bell Telephone Laboratories, Inc., Murray Hill, New Jersey, 1964.
2. J. DeKlerk and E. F. Kelly, "Coherent Phonon Generation with Gigacycle Range via Insulating Cadmium Sulfide Films," Appl. Phys. Letters 2, 2 (1 July 1964); J. DeKlerk, Paper presented at IEEE Sonics and Ultrasonics Symposium, Oct. 14-16, 1964, Santa Monica, Calif.
3. F. H. Pizzarello, "CdS Thin-Film Formation by the Method of Co-evaporation," J. Appl. Phys. 35, 2730 (September 1964); Hughes Aircraft Co., Semiconductor Division, Newport Beach, Calif.

Unclassified

Security Classification

DOCUMENT CONTROL DATA - R&D		
<i>(Security classification of title, body of abstract and indexing annotation must be entered when the overall report is classified)</i>		
1. ORIGINATING ACTIVITY (Corporate author) W. W. Hansen Laboratories of Physics Microwave Laboratory Stanford University		2a. REPORT SECURITY CLASSIFICATION Unclassified
		2b. GROUP
3. REPORT TITLE  MULTIMEGAWATT BROADBAND MICROWAVE TUBES, THIRD ANNUAL REPORT		
4. DESCRIPTIVE NOTES (Type of report and inclusive dates) Final Report, 1 Nov 63 - 31 Oct 64		
5. AUTHOR(S) (Last name, first name, initial) Not Given. Responsible Investigator on Contract: Chodorow, Marvin		
6. REPORT DATE March 1965	7a. TOTAL NO. OF PAGES 58	7b. NO. OF REFS 13
8a. CONTRACT OR GRANT NO. AF30(602)-2575	9a. ORIGINATOR'S REPORT NUMBER(S) M. L. Report No. 1264	
b. PROJECT NO. 5573		
c. Task No. 557303	9b. OTHER REPORT NO(S) (Any other numbers that may be assigned this report) RADC-TR-64-583	
d.		
10. AVAILABILITY/LIMITATION NOTICES Qualified requestors may obtain copies of this report from DDC. Release to OTS is authorized.		
11. SUPPLEMENTARY NOTES	12. SPONSORING MILITARY ACTIVITY Rome Air Development Center Griffiss AFB New York	
13. ABSTRACT The report summarizes the contract year. Individual abstracts for each task are as follows: I. <u>Extended Interaction Klystrons</u> : The small signal performance of a three-cavity extended interaction klystron operating in conjunction with the electron kick at 25 Kv, 1100 Mc is presented. II. <u>Centipede TWT</u> : Amplitude and phase characteristics within the coupled cavities are presented. III. <u>Transverse Wave Studies</u> : An analytical analysis of transverse wave propagation on an accelerated beam in an axially magnetic field is presented. IV. <u>Whistler Mode Propagation in Solids</u> : Preliminary calculations and discussion are presented. V. <u>Carrier Wave Propagation in Solids</u> : Preliminary results on a study of the Gunn effect are presented. VI. <u>Acoustic Wave Devices</u> : Progress in thin film coupler techniques is presented.		

DD FORM 1473  
1 JAN 64

UNCLASSIFIED

Security Classification

14. KEY WORDS	LINK A		LINK B		LINK C	
	ROLE	WT	ROLE	WT	ROLE	WT
Traveling Wave Tube Circuits Extended Interaction Klystrons Transverse Wave Devices Solid State Plasma Devices Acoustic Wave Devices						

**INSTRUCTIONS**

1. **ORIGINATING ACTIVITY:** Enter the name and address of the contractor, subcontractor, grantee, Department of Defense activity or other organization (corporate author) issuing the report.
- 2a. **REPORT SECURITY CLASSIFICATION:** Enter the overall security classification of the report. Indicate whether "Restricted Data" is included. Marking is to be in accordance with appropriate security regulations.
- 2b. **GROUP:** Automatic downgrading is specified in DoD Directive 5200.10 and Armed Forces Industrial Manual. Enter the group number. Also, when applicable, show that optional markings have been used for Group 3 and Group 4 as authorized.
3. **REPORT TITLE:** Enter the complete report title in all capital letters. Titles in all cases should be unclassified. If a meaningful title cannot be selected without classification, show title classification in all capitals in parentheses immediately following the title.
4. **DESCRIPTIVE NOTES:** If appropriate, enter the type of report, e.g., interim, progress, summary, annual, or final. Give the inclusive dates when a specific reporting period is covered.
5. **AUTHOR(S):** Enter the name(s) of author(s) as shown on or in the report. Enter last name, first name, middle initial. If military, show rank and branch of service. The name of the principal author is an absolute minimum requirement.
6. **REPORT DATE:** Enter the date of the report as day, month, year, or month, year. If more than one date appears on the report, use date of publication.
- 7a. **TOTAL NUMBER OF PAGES:** The total page count should follow normal pagination procedures, i.e., enter the number of pages containing information.
- 7b. **NUMBER OF REFERENCES:** Enter the total number of references cited in the report.
- 8a. **CONTRACT OR GRANT NUMBER:** If appropriate, enter the applicable number of the contract or grant under which the report was written.
- 8b, 8c, & 8d. **PROJECT NUMBER:** Enter the appropriate military department identification, such as project number, subproject number, system numbers, task number, etc.
- 9a. **ORIGINATOR'S REPORT NUMBER(S):** Enter the official report number by which the document will be identified and controlled by the originating activity. This number must be unique to this report.
- 9b. **OTHER REPORT NUMBER(S):** If the report has been assigned any other report numbers (either by the originator or by the sponsor), also enter this number(s).
10. **AVAILABILITY/LIMITATION NOTICES:** Enter any limitations on further dissemination of the report, other than those

imposed by security classification, using standard statements such as:

- (1) "Qualified requesters may obtain copies of this report from DDC."
- (2) "Foreign announcement and dissemination of this report by DDC is not authorized."
- (3) "U. S. Government agencies may obtain copies of this report directly from DDC. Other qualified DDC users shall request through \_\_\_\_\_."
- (4) "U. S. military agencies may obtain copies of this report directly from DDC. Other qualified users shall request through \_\_\_\_\_."
- (5) "All distribution of this report is controlled. Qualified DDC users shall request through \_\_\_\_\_."

If the report has been furnished to the Office of Technical Services, Department of Commerce, for sale to the public, indicate this fact and enter the price, if known.

11. **SUPPLEMENTARY NOTES:** Use for additional explanatory notes.
12. **SPONSORING MILITARY ACTIVITY:** Enter the name of the departmental project office or laboratory sponsoring (paying for) the research and development. Include address.
13. **ABSTRACT:** Enter an abstract giving a brief and factual summary of the document indicative of the report, even though it may also appear elsewhere in the body of the technical report. If additional space is required, a continuation sheet shall be attached.

It is highly desirable that the abstract of classified reports be unclassified. Each paragraph of the abstract shall end with an indication of the military security classification of the information in the paragraph, represented as (TS), (S), (C), or (U).

There is no limitation on the length of the abstract. However, the suggested length is from 150 to 225 words.

14. **KEY WORDS:** Key words are technically meaningful terms or short phrases that characterize a report and may be used as index entries for cataloging the report. Key words must be selected so that no security classification is required. Identifiers, such as equipment model designation, trade name, military project code name, geographic location, may be used as key words but will be followed by an indication of technical context. The assignment of links, roles, and weights is optional.